

The Joy of Markov Models—Channel Gating and Transport Cycling Made Easy

G. Zifarelli¹, P. Zuccolini¹, S. Bertelli^{1,2}, M. Pusch^{1*}

¹Istituto di Biofisica, Consiglio Nazionale delle Ricerche, Via De Marini 6, I-16149 Genova, Italy

²Scuola Internazionale Superiore di Studi Avanzati, I-34136 Trieste, Italy

ABSTRACT The behavior of ion channels and transporters is often modeled using discrete state continuous-time Markov models. Such models are helpful for the interpretation of experimental data and can guide the design of experiments by testing specific predictions. Here, we describe a computational tool that allows us to create Markov models of chosen complexity and to calculate the predictions on a macroscopic scale, as well on a single-molecule scale. The program calculates steady-state properties (current, state probabilities, and cycle frequencies), deterministic macroscopic and stochastic time courses, gating currents, dwell-time histograms, and power spectra of channels and transporters. In addition, a visual simulation mode allows us to follow the time-dependent stochastic behavior of a single channel or transporter. After a basic introduction into the concept of Markov models, real-life examples are discussed, including a model of a simple K⁺ channel, a voltage-gated sodium channel, a 3-state ligand-gated channel, and an electrogenic uniporter. In this manner, the article has a modular architecture, progressing from basic to more advanced topics. This illustrates how the MarkovEditor program can serve students to explore Markov models at a basic level but is also suited for research scientists to test and develop models on the mechanisms of protein function.

KEY WORDS ion channels; computational modeling; student learning

I. GENERAL MOTIVATION

At a molecular level, diffusion of substrates and macromolecules combined with conformational changes of proteins underlie most biologic processes. Even though these molecular events are not occurring in thermodynamic equilibrium, they are actually in most cases not far from equilibrium. In general, processes that occur close to thermodynamic equilibrium are energetically favorable compared with processes far from equilibrium. Indeed, energetic efficiency is one of the major drivers of evolution (1). An instructive example is the energy consumption of the human brain compared with that of human-made computers. The brain's computational power has been estimated to be above the most potent presently available supercomputers (2).

Despite this capacity, the energy demand of the human brain corresponds to only roughly 20 W, i.e., less than a conventional (old-fashioned) light bulb. In contrast, a typical supercomputer consumes on the order of megawatts, i.e., many orders of magnitude more. One of the reasons behind the incredible efficiency of the brain is that the mechanisms of biologic data processing operate rather close to

“*” corresponding author

Received: 12 December 2019
Accepted: 30 September 2020
Published: 30 March 2021

© 2021 Biophysical Society.

thermodynamic equilibrium. The free energy differences between the various conformations of proteins are of the order of a few kT . The free energy corresponding to $1 kT$ is the energy that can be easily surmounted by random movements in thermal equilibrium. In terms of equivalent electrical voltage, kT corresponds to $\sim 0.025 \text{ V} = 25 \text{ mV}$ (i.e., $kT/q_e \sim 25 \text{ mV}$ at physiologic temperatures, where q_e is the absolute electrical charge of an electron). This is a much smaller value than the operating voltage of transistors in computers, which is of the order of $\sim 3,000 \text{ mV} = 120 kT/q_e$. Because the probability of a reaction depends in an exponential manner on the free energy difference (between initial and final states), a value of $120 kT$ assures almost 100% deterministic operation, but on the downside, it is paid for with a large power consumption. In contrast, biologic processes are mostly not deterministic but often rely on redundancy to assure approximate accuracy. There are, of course, many exceptions to this simplified view. For example, for voltage-gated cation channels, whose opening transition is accompanied by the translocation of up to 13 elementary charges, the free energy difference upon a potential shift of 75 mV will amount to $75 \text{ mV} \times 13 q_e$, corresponding to $39 kT$.

Even though, theoretically, proteins can exist in a practically unlimited number of conformations (or microstates), in many cases their enzymatic function can be described in terms of a limited number of states that correspond to an ensemble of microstates with similar conformation. A classic example is an enzyme that binds and transform a single substrate (Fig 1A). The cartoon in Figure 1A is clearly simplified, but it could provide more than a qualitative description of enzyme function. Indeed, the scheme of Figure 1A could be used, in principle, to generate a precise mathematic description of how the enzymatic activity depends on the concentration of substrates, conformational changes of the enzyme, and other factors.

A problem is that most biophysical and biochemical methods yield information on the average behavior of the ensemble of a large

number of identical or similar molecules but do not capture the behavior of single molecules. In 1976, the patch-clamp technique and bilayer recordings allowed one for the first time to observe the function of a single biologic molecule in real time (3, 4). Figure 1B shows a typical single-channel recording from skeletal muscle: the openings and closings of a single acetylcholine receptor channel in the presence of 50 nM of suberyldicholine are clearly visible (5). Since these early experiments, the patch-clamp method was quickly adopted in many laboratories worldwide and led to the discovery of a plethora of different ion channels present in practically all cell types (6).

Detailed analysis of single-channel recordings revealed 2 important properties: the channels switch between distinct conductance states in a very short time (too short to be measurable by the patch-clamp technique) and the distribution of the dwell times in these conductance states can be very well described by exponential distributions. This is illustrated in Figure 1C for a hypothetical ion channel with 2 closed states and 1 open state. The histogram of all open-channel events is well described by a single exponential distribution, whereas the histogram of the closed-channel events is well-fitted by a double exponential function (see pink curves in Fig 1C). In fact, very often the dwell-time distribution of shut (not conducting) periods shows a complex multiexponential distribution, originating from conformational changes occurring before channel opening. These conformational changes cannot be detected by changes of the current amplitude but can be indirectly inferred from the kinetic analysis. As will be explained in more detail in the following, these properties are very well described by a so-called time homogeneous Markov process. The defining feature of a Markov process is the lack of memory: the probability that a state transition (e.g., from closed to open) happens does not depend on how much time the channel has spent in the previous conformation. This concept will be explained in more detail later.

These rather general considerations explain why to obtain a mechanistic insight into a

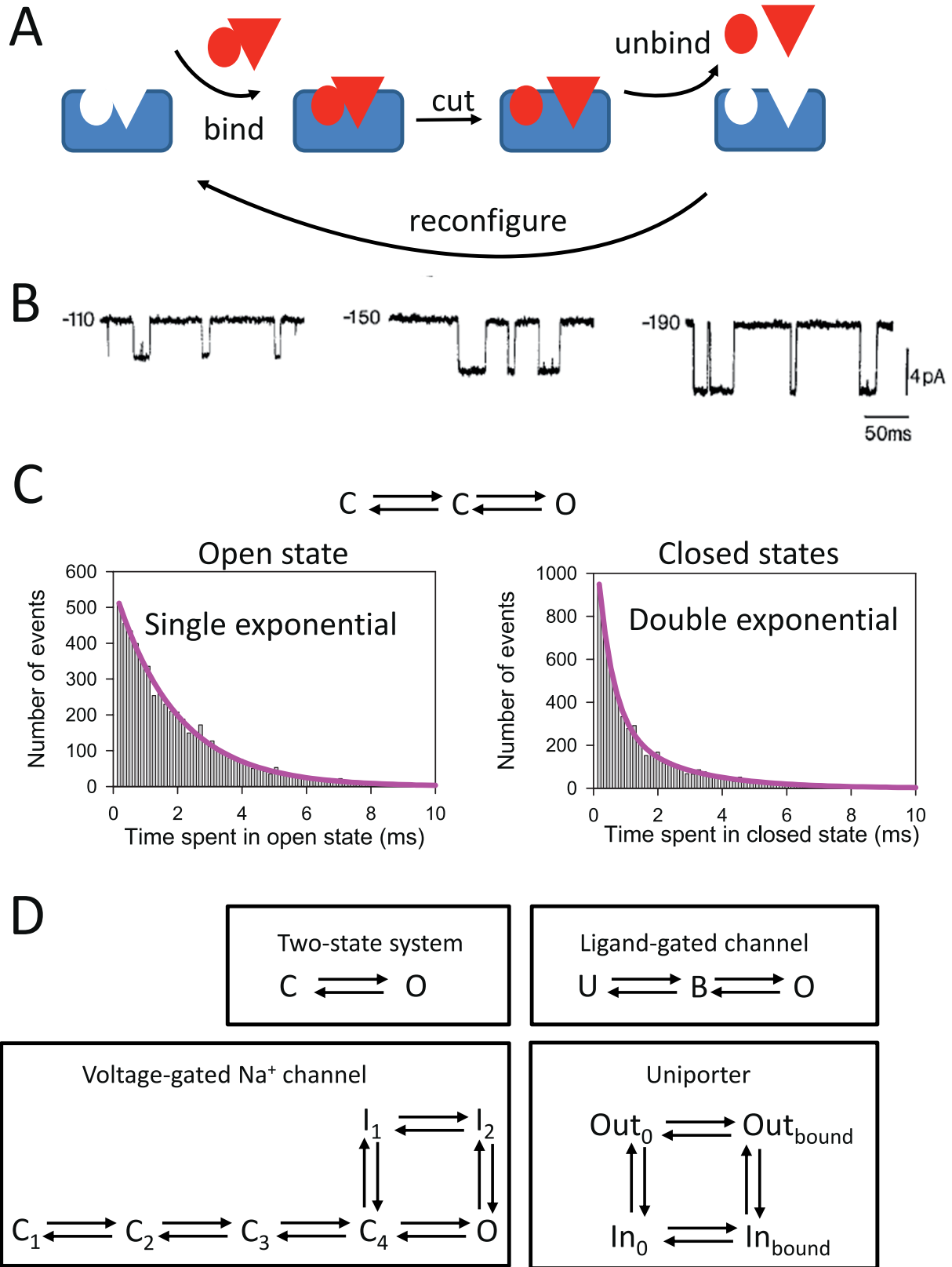


Fig 1. Principles of enzyme and ion channel function. In (A) the cartoon depicts the reaction steps of a hypothetical enzyme that binds a substrate, cuts it, and then releases 2 products. (B) Single-channel traces of an acetylcholine receptor at various voltages are shown (4). (C) This illustrates the typical dwell-time distributions of a 3-state system with 2 closed states and 1 open state, in which the open dwell-time distribution is well fitted by a single exponential function (left, pink line), while the closed state histogram requires the sum of 2 exponential functions (right, pink line). The histograms were generated by MarkovEditor and a simple 3-state system. (D) All examples of Markov models are explained in more detail in the present article.

complex biologic process. It is essential to study the individual components of the system in isolation and under controlled conditions that bring them close to thermodynamic equilibrium. A prominent example is the propagation of electrical signals along the sometimes extremely long processes of nerve cells (axons), which has attracted considerable attention among physiologists in the past century. In particular, the studies of Hodgkin and Huxley on the basis of the generation and propagation of the neuronal “action potential” (6, 7) have paved the way for a detailed, mechanistic investigation of the molecular basis of electrical excitability. The action potential is an explosive change of the cellular membrane potential from a normally negative value (around -70 mV) to a positive value (around 40 mV, a process called *depolarization*) within roughly a millisecond, followed by a slightly slower repolarization of the membrane potential to the resting value of -70 mV. In nerve axons, that connect, for example, the brain to motor neurons and drive muscle contraction, the action potential travels as an excitatory wave at high speed toward the target neuron or muscle. The mechanisms underlying action potential generation and propagation have been described in terms of probabilistic discrete state continuous-time (i.e., Markov) models in a groundbreaking publication by Hodgkin and Huxley in 1952 (7). Intriguingly, this approach allowed for the laying out the mechanistic underpinning of the action potential 50 years before the three-dimensional structure of the ion channels involved was available (8, 9). The neuronal action potential is driven by the opening of ion channels in the nerve membrane. Voltage-gated Na^+ channels underlie the initial depolarization. The reason for the depolarization is that the extracellular Na^+ concentration is much higher than the intracellular Na^+ concentration. Therefore, opening of Na^+ channels leads to a Na^+ influx at voltages more negative than the Na^+ equilibrium potential, which is around $+50$ mV, i.e., much higher than normal membrane potentials. After the upstroke of the action potential, the combined effect of

Na^+ channel inactivation, presence of background K^+ channels, and the delayed opening of voltage-gated K^+ channels results in the repolarization of the membrane potential. The reason why K^+ channels repolarize the membrane potential is that extracellular K^+ is much lower than intracellular K^+ . Therefore, at voltages more positive than about -80 mV, the K^+ equilibrium voltage in most cells, K^+ efflux occurs upon opening of K^+ channels.

On a historical note, Hodgkin and Huxley were not aware of the mechanistic value of the theory in terms of conformational change of proteins. Yet, the idea of probabilistic gates regulating opening of the voltage-gated ion channels continues to be highly relevant for the understanding of ion channel and enzyme function in general.

Typical schemes of Markov models used to describe channel gating and transporter function are illustrated schematically in Figure 1D, which shows the Markov models discussed in the present article. The various states of the model are connected by rate constants (indicated by arrows), whose meaning will be defined in detail in the next section. The general mathematic treatment of such Markov models has been covered in several excellent publications (10), which are highly recommended for the interested reader. For a basic usage of MarkovEditor (<http://users.ge.ibf.cnr.it/pusch/sframes/StateEditor.html>), such deep knowledge is not strictly necessary but is certainly useful. In mathematic terms, Markovian systems respond in a relatively simple manner to an external perturbation, as, for example, a change in membrane potential or ligand concentration. The time-dependent relaxation of the occupation probabilities of the various states upon perturbation of a Markov model is provided by the sum of n exponential functions, where $n = \text{Number of states} - 1$, and where the time constants of the exponentials are the eigenvalues of the so-called Q matrix of the rate constants (10–12). For example, the relaxation of a 3-state voltage-gated channel upon a voltage jump is described by a double-exponential function. Most electrophysiologists know very well that it is

extremely difficult to extract more than 2 time-constants from a given dataset. Thus, it may seem that Markov models with more than 3 states might be rather useless in practical terms. Nevertheless, a priori knowledge of the possible physical states of the system, combined with symmetry arguments, can provide deep insight into the molecular machinery of the channel or transporter of interest. Moreover, due to the mathematic complexity of the problem, for systems with more than 2 states, it is very difficult to understand at the intuitive level how changes of any rate constant affect the macroscopic properties.

II. TARGET AUDIENCE AND OUTLINE OF THE ARTICLE

The present article aims to provide a rather intuitive tool, accessible to a wide readership, to explore simple and complex Markov models, allowing to directly simulate the effect on channel or transporter behavior caused by changes of any microscopic parameter, both at the single-channel level, as well as at the ensemble level. The article is organized such that the different applications of the computational tool MarkovEditor are presented as blocks of increasing complexity. This is done in different, self-contained paragraphs such that the reader can choose the sections with the appropriate level.

Our idea is that this software and the relative tutorials are most useful for people who already have some background knowledge on ion channels or transporters and who desire a tool to be guided into the quantitative study of various specific aspects. A deep understanding of single-channel behavior might be more difficult to achieve based solely on the more commonly studied properties of macroscopic currents explained, for example, in a university physiology course. The expected users of MarkovEditor are indeed master's students, master's student interns, PhD students or early postdoctoral students rather than complete beginners such as bachelor students. The concept is to help them visualize how the theory, summarized in

equations, can actually describe a channel's behavior and what is the impact of some parameters, such as a rate constant, on the final current. This can be seen both at the single channel and the whole-cell level. We envision some teaching-scenarios, in which such a tool can be useful. A possible situation is when a principal investigator (PI) wishes to introduce into the world of Markov models PhD students or early postdoctoral students, who have worked only with whole-cell currents. The PI, or more experienced members of the lab crew, could be available for guidance, when required. The software can also be used by professors teaching in advanced courses: the lecturer could go through the theoretic aspects step by step, while showing models and simulations with MarkovEditor. In this case, the software and the present article can also be used for home exercises, to practice on concepts introduced during class. Another situation in which MarkovEditor might be helpful are practical courses, in which a group of students rotate in a lab, where single-channel experiments are routinely performed. MarkovEditor could be used to explain what they are going to see in the following weeks and what is the meaning of the data analysis they will be required to do. Finally, MarkovEditor can be a useful tool for active scientists working on transporters or channels or are using other single-molecule approaches.

We should not forget to mention that other Markov modeling software is freely available. The most prominent are QuB (<https://qub.mandelics.com/>) and programs from the HJCFit suite (<https://dcprogs.github.io/HJCFITdevdocs/>). The scope of these programs is, however, quite different from that of MarkovEditor. HJCFit programs are highly specialized for professional single-channel data analysis, including missed events correction (13). QuB has overlap with MarkovEditor but lacks several features, such as transport cycle analysis, varying parameters, and others. However, the reader should consult the corresponding Web sites to find out more detail on these programs.

III. THE 2-STATE MODEL

Before delving into complex models, we will discuss the simplest possible Markov model, the 2-state system (Fig 2A,B). We will first describe the fundamental mathematics of the system, defining the concept of rate constants and highlighting the essential feature on any Markovian system: the lack of memory. We will then use the 2-state system to introduce most features of the MarkovEditor program.

The 2-state system is schematically depicted in this (apparently innocent) scheme:



At any given thermodynamic condition, defined by membrane voltage, pressure, temperature, or concentration of ligands, this 2-state system is characterized by 2 numbers: the opening rate constant α and the closing rate constant β (Fig 2A). The basic assumptions underlying this simplified description are

- the channel can be either in state *O* (open) or in state *C* (closed; i.e., there are no intermediate configurations),
- transitions between states occur abruptly, and
- the channel is completely memoryless.

The latter assumption is what defines Markov systems and means that after a transition to a new state has occurred, the probability that a further transition takes place, is independent of how much time the channel has already spent in the current state. Only with this assumption the following definition of the rate constants α and β makes sense: Given a very small time interval dt and given that the channel is in state *C* at time t , the probability that it makes a transition to state *O* between t and $t + dt$ is equal to

$$P(O, t + dt|C, t) = \alpha dt \quad (2)$$

Here, the notation of conditional probability is used, i.e., $P(A|B)$ means probability of *A*, given that *B* is true. Thus, $P(O, t + dt|C, t)$ is the probability to find the channel in state *O* at time $t + dt$, knowing that it was in state *C* at

time t . The probability of this transition is proportional to the time lag dt (as long as it remains very small) and proportional to the opening rate constant α . Thus, α provides the speed with which the channel switches to state *O*.

Similarly, the closing rate constant β is defined by

$$P(C, t + dt|O, t) = \beta dt \quad (3)$$

These equations are valid for infinitesimal times dt . To deal with longer times, we will need the concept of a differential equation as described below.

The Markov property of lack of memory implies that the transition probability is independent of t and can thus be expressed as

$$P(O, t + dt|C, t) = P(O, dt|C, 0) = \alpha dt \quad (4)$$

i.e., knowing that the channel is closed at time 0, the probability to find it open after time dt is equal to αdt .

The opening and closing rate constants define the rate at which the system can surmount the energy barrier between the 2 states, as illustrated in Figure 2B. One can envision the system undergoing thermal fluctuations, attempting continuously to overcome the barrier characterized by a certain activation energy, E_a . Only occasionally has the system enough energy to surmount the barrier. This probability depends in an exponential manner on the activation energy (14). Most importantly, the transition probability is independent of how long the channel has already been in a given state.

These mathematic properties imply that $P_O(t)$ and $P_C(t)$, i.e., the time-dependent state probabilities, obey the following fundamental linear differential equations:

$$\frac{dP_O(t)}{dt} = -\alpha P_O(t) + \beta P_C(t) \quad (5)$$

and

$$\frac{dP_C(t)}{dt} = \alpha P_O(t) - \beta P_C(t) \quad (6)$$

Differential equations as these relate the rate of change of a quantity (i.e., its temporal

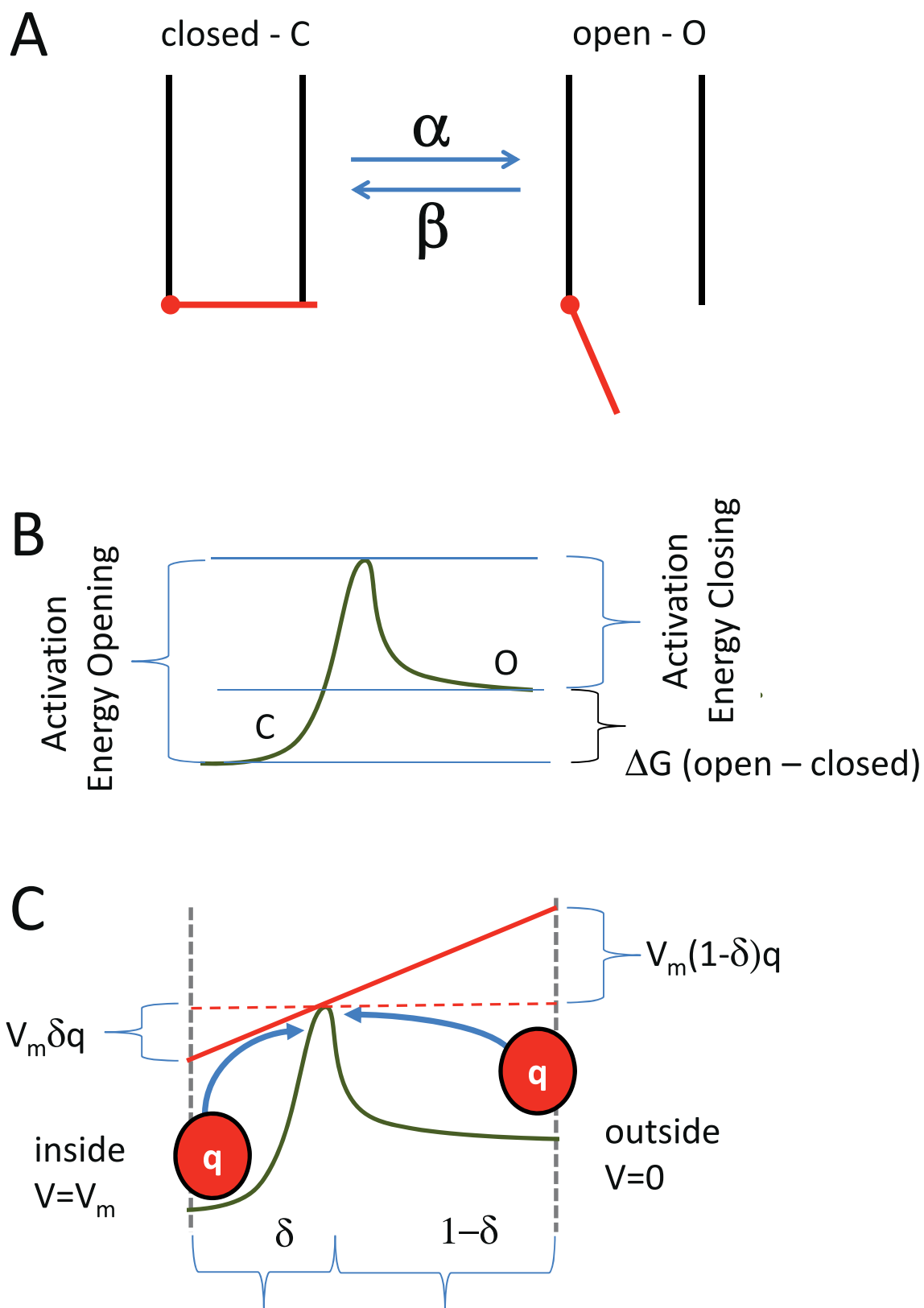


Fig 2. The 2-state model. (A) The cartoon depicts 2 configurations of an ion channel, closed (left) and open (right) with the rate constants α and β relative to the 2 transitions. (B) A hypothetical activation energy profile connecting the 2 states is illustrated. (C) The concept of a gating charge and the electrical distance δ is shown (see text for details).

derivative) to the value of the quantity itself. The previously mentioned equations are in essence equivalent to those used to describe chemical reactions by the law of mass action. For example, the isomerization of a compound from a *cis* to a *trans* conformation would be described by a completely equivalent set of differential equations.

Note that summing Eqs. 5 and 6 yields

$$\frac{dP_O(t)}{dt} + \frac{dP_C(t)}{dt} = 0 \quad (7)$$

ensuring that the total probability to be in any state remains constant and equal to 1.

In fact, for the 2-state model

$$P_O(t) + P_C(t) = 1 \quad (8)$$

i.e., the channel has only 2 possibilities, to be either in the closed or open state. Thus, $P_C(t)$ can be substituted by

$$P_C(t) = 1 - P_O(t) \quad (9)$$

Inserting this substitution into (Eq. 5), i.e., replacing $P_C(t)$ by $1 - P_O(t)$, leads to the following linear differential equation of the single function $P_O(t)$:

$$\frac{dP_O(t)}{dt} = -(\alpha + \beta)P_O(t) + \beta \quad (10)$$

This differential equation determines the response of the 2-state system to a perturbation, which could be a change in voltage or a change in the concentration of a ligand. Upon the perturbation, the system relaxes to a new steady state, determined by the altered opening or closing rate constants, according to the fundamental time-dependent single-exponential solution

$$P_O(t) = \frac{\alpha}{\alpha + \beta} + \left(P_O^0 - \frac{\alpha}{\alpha + \beta} \right) e^{-(\alpha + \beta)t} \quad (11)$$

Here, P_O^0 is the initial open probability at time 0 (assumed to be known). It is instructive to verify that this is indeed a solution of the differential equation (Eq. 10), with the initial condition $P_O(0) = P_O^0$. At infinite time, which corresponds to a true equilibrium in this case, P_O reaches the steady-state value

$$P_O(\infty) = \frac{\alpha}{\alpha + \beta} \quad (12)$$

The relaxation from the initial state to the final equilibrium occurs with the time constant

$$\tau = \frac{1}{\alpha + \beta} \quad (13)$$

Thus, using a slightly different notation, the fundamental solution (Eq. 11) can also be written as

$$P_O(t) = P_O(\infty) + (P_O^0 - P_O(\infty))e^{-\frac{t}{\tau}} \quad (14)$$

and similarly one obtains

$$P_C(t) = P_C(\infty) + (P_C^0 - P_C(\infty))e^{-\frac{t}{\tau}} \quad (15)$$

Before inserting this 2-state model into the MarkovEditor program for further exploration, we will endow it with a typical voltage dependence of the rate constants, a property that is fundamental for electrical excitation in neurons but also important in many electrogenic transporters. In voltage-gated cation channels, highly specialized electrically charged segments of the channel proteins, the so-called voltage sensors, move within the electric field across the membrane upon a change of the membrane voltage (6). In the simple 2-state model, voltage sensor movement and channel opening occur simultaneously, i.e., they are perfectly coupled. This is not fully realistic but useful to illustrate the basic concept. As depicted in Figure 2C, the gating charge q , associated with voltage sensor movement, can be either close to the inside of the membrane (in the closed state) or close to the outside (in the open state), providing stabilization of the open state at positive membrane voltages. It is convenient to express the gating charge of a single channel in terms of the absolute elementary charge of an electron, $q_e = 1.602 \times 10^{-19}$ C, i.e.,

$$q = zq_e \quad (16)$$

introducing the gating valence z . The rate constants depend in an exponential manner on the membrane potential V and on the gating charge in the following manner

$$\alpha(V) = \alpha_0 e^{\delta z V q_e / (kT)} \quad (17)$$

and

$$\beta(V) = \beta_0 e^{-(1-\delta)zVq_e/(kT)} \quad (18)$$

These equations are crucial for all models discussed in this article: α_0 and β_0 are the respective opening and closing rate constants at a membrane potential of 0 mV, k is the Boltzmann constant, q_e the (absolute) charge of an electron, and T the absolute temperature. The relative apparent electrical distance δ takes into account a possible asymmetric dependence of the rate constants on voltage (see Fig 2C). For a more elementary introduction into the concept of electrical distance, the reader is referred to (6). The exponential voltage dependence of the rate constants is based on transition state theory, which cannot be explained in detail here; see (14). Briefly, as explained previously, the speed of a conformational change is determined by the activation energy. In addition to the conformational energy (expressed in terms of α_0 and β_0), for a voltage-dependent transition, the activation energy includes the energy that has to be provided to move the gating charge along a certain fraction of the electric field across the membrane (see Fig 2C). For opening transition, this fraction is given by δ and for the closing transition by $1 - \delta$. Note that Figure 2C makes the simplifying assumption that the gating charge moves all the way from the inside to the outside during opening. If it moved only part of the distance, the effective gating valence would be proportionally reduced. In Eqs. 17 and 18, at physiologic temperatures, the factor $kT/q_e \sim 25$ mV, and thus if V is measured in millivolts, the previous equations can also be written more simply as

$$\alpha(V) = \alpha_0 e^{\delta zV/25} \quad (19)$$

$$\beta(V) = \beta_0 e^{-(1-\delta)zV/25} \quad (20)$$

a form that for simplicity will be used in the models described in the present article. In case the temperature is considered an important variable, the equations can be adjusted accordingly. It can be seen that the gating of the voltage-dependent 2-state system depends on exactly 4 parameters: α_0 and β_0 , the rate

constants at 0 mV; z , the gating valence; and δ , the relative electrical distance associated with opening.

The steady-state voltage dependence of the open probability turns out to be

$$\begin{aligned} P_O(V) &= \frac{\alpha(V)}{\alpha(V) + \beta(V)} = \frac{1}{1 + e^{-z\left(V-V_{1/2}\right)q_e/(kT)}} \\ &= \frac{1}{1 + e^{-z\left(V-V_{1/2}\right)/25}} \end{aligned} \quad (21)$$

where $V_{1/2}$, the voltage of half-maximal activation ($P_O(V_{1/2}) = 0.5$) depends only on α_0/β_0 . Importantly, $P_O(V)$ is independent of δ . This equation is also called a *Boltzmann distribution*, because it fundamentally derives from the classical Boltzmann statistics describing systems in thermodynamic equilibrium.

Relaxation time constants are given by

$$\begin{aligned} \tau(V) &= \frac{1}{\alpha(V) + \beta(V)} \\ &= \frac{1}{\alpha_0 e^{\delta zV/25} + \beta_0 e^{-(1-\delta)zV/25}} \end{aligned} \quad (22)$$

Finally, the total predicted ion current of a channel model depends of the possibly voltage-dependent single-channel ion currents associated with each conducting state. For the 2-state model, we will assume a linear current voltage relationship characterized by the single-channel conductance γ and the reversal potential E_{rev}

$$i(V) = \gamma(V - E_{rev}) \quad (23)$$

To simulate a classical K^+ channel, we assume, for example, $E_{rev} = -80$ mV, similar to a neuronal potassium channel. Further properties of the 2-state system will be discussed within the MarkovEditor tool in the next section.

IV. THE TIME DEPENDENCE: MACROSCOPIC AND MICROSCOPIC RELAXATIONS

Tutorial 2 describes how to insert the 2-state model into MarkovEditor, and in the following, we will assume that this step is complete.

We will verify if MarkovEditor reliably reproduces the previously described general properties and explore the dependence on the various parameters of the model. Predictions of model calculations are shown in the upper panel on the left of MarkovEditor, and calculations are invoked by clicking on the `Calculate` button. To simulate the temporal development, either at the macroscopic or at the single-channel level, we have to impose a voltage protocol, emulating the typical stimulation protocols used in electrophysiologic measurements. MarkovEditor offers 2 alternative stimulation protocols:

- (a) A simple protocol consisting of 3 stimulation segments is defined in the `General Settings` (see Tutorial 3 for a more exhaustive description of the `General Settings`).
- (b) More complex stimulation protocols can be defined by using the `Pulse Generator File` paradigm, explained in more detail in Tutorial 4.

Let us use the simple 3 stimulation segments protocol to simulate the response of the 2-state model to a single voltage step. For this, using the menu item `Settings->Edit general settings`, we select `NPulses = 1; sample time = 0.1; VHold = -100, t0 = tHold = 50; V1 = -20, t1 = 500; V2 = -80, t2 = 200` (the delta values are irrelevant if only a single pulse is simulated). The corresponding settings file `2States.set` can be downloaded from <https://github.com/mikpusch/MarkovEditor.git>. This protocol is a standard pulse used to examine the behavior of classical voltage-gated ion channels. The holding voltage of -100 mV is, on the one hand, close to the physiologic resting membrane potential of many excitable cells and, on the other hand, guarantees that the initial open probability is relatively small (for our 2-state system). To invoke the simulation by MarkovEditor, we first select the radio button `Current` in the `Time course` tab and then click on the `Calculate` button to trigger the calculation shown in the graph on the top left (Fig 3A). The graph offers several display options and data can be easily exported, as

described in Tutorial 5. We see that the initial negative holding current at -100 mV is very small, because the open probability is only 0.33%. Stepping the voltage to -20 mV leads to an exponential increase of the outward potassium current, which reaches almost steady state during the 500-ms pulse. Upon returning the voltage to -100 mV, the initial tail current is relatively large, reflecting the initial sizable open probability of 65%, reached at the end of the preceding pulse to -20 mV, decaying back to the holding current, again with an exponential time course. Selecting the `Prob` radio button, displays the time course of the occupation probabilities of the closed state (in black) and the open state (in red; not depicted). By playing with the various options offered by the stimulation protocols, the macroscopic relaxations of the 2-state model can be explored in an exhaustive manner.

V. STOCHASTIC SIMULATIONS OF SINGLE CHANNELS

We next explore the stochastic response of a single channel to the very same stimulation protocol described previously. To render the response more realistic, we artificially assign a noise level to both the open as well as to the closed state. This is done by double-clicking or right-clicking on each state and assigning the noise level (`sigma`). In this manner, the current is associated with random noise with a standard deviation defined here. Note that before the setting of the noise, the user is asked to enter the label of the state and the current associated with it. This noise is typical for single-channel recordings and reflects noise caused by a finite seal resistance, amplifier noise, or stray capacitance (11). For the closed state, we select `sigma = 0.05 pA`, whereas for the open state, we select higher noise level of `0.1 pA`, reflecting the observation of open channel noise (15). Now, we select the radio button `Current` from the `Simulation` tab. Each time the `Calculate` button is clicked, the program simulates and shows the response of a single channel. As illustrated in Figure 3B, the stochastic behavior of the channel implies

Ensemble

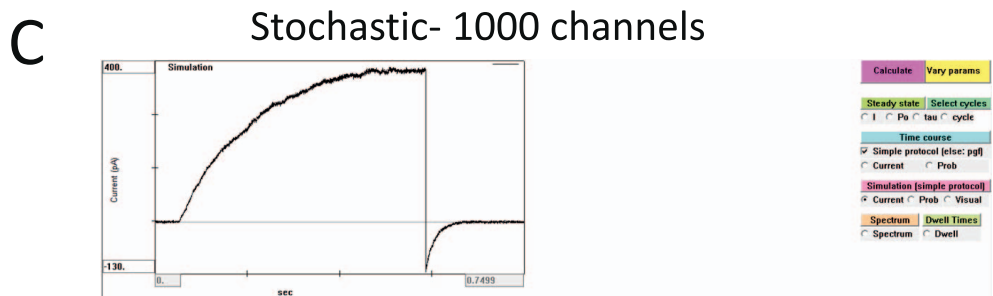
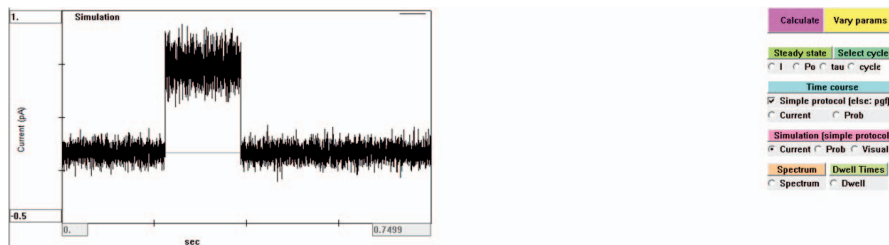
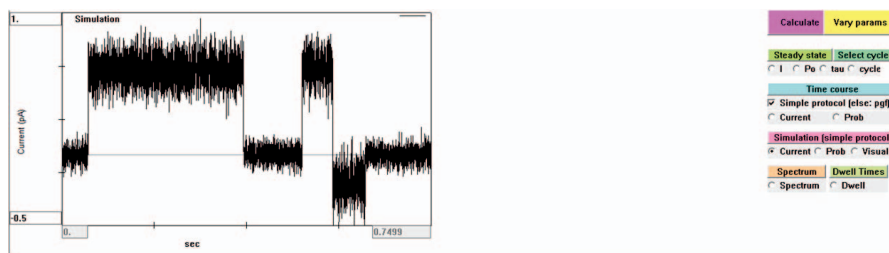
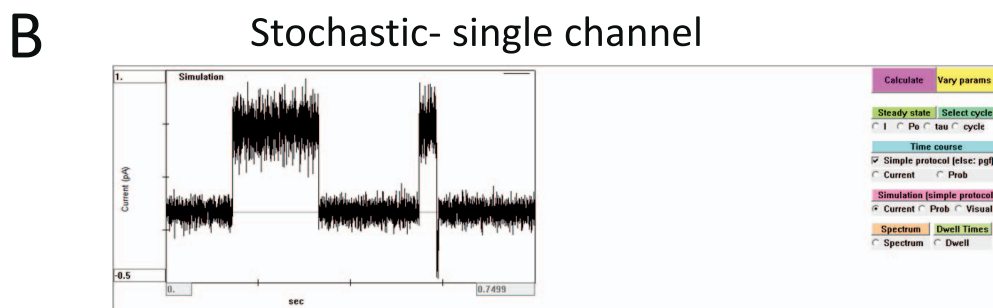
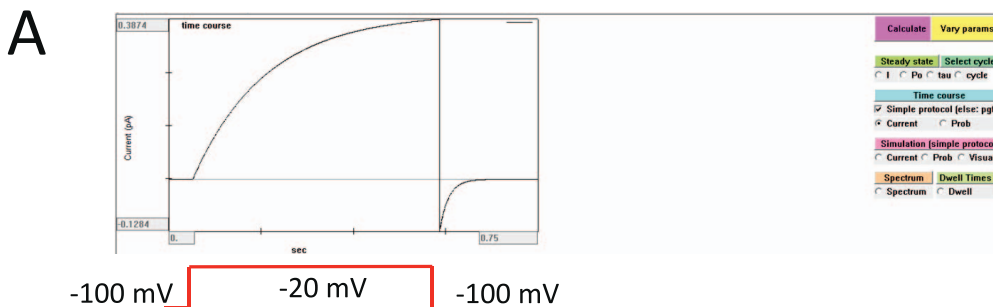


Fig 3. Ensemble and stochastic time-dependent simulation. For the 2-state model, the response to a step depolarization to -20 mV from a holding potential of -100 mV is calculated at the ensemble (i.e., deterministic) level (A), with the pulse protocol illustrated in red, in a stochastic manner for a single channel (B), or in a stochastic manner for 1,000 channels (C). For the stochastic simulations (B and C), noise levels of 0.05 pA (Gaussian white noise) for the closed state and 0.1 pA for the open state, respectively, were added to render the single-channel events realistic.

that the response is slightly different in the 3 simulations, even if the parameters are exactly the same. For a quantitative understanding of the behavior of the single channel, it might be insightful to select a large number of pulses in the `General Settings` dialog, export the data, and perform single-channel analysis with a program of choice. This procedure is also helpful to assure the accuracy of any chosen analysis procedure.

VI. COMPARING DETERMINISTIC AND STOCHASTIC PREDICTIONS

Another instructive exercise is to compare the stochastic predictions of the model with the macroscopic, deterministic behavior. To this end, we can assign a large number of channels to be simulated in the `GeneralSettings` dialog, for example, `No. Channels in stochastic simulations = 1000`. Under these conditions, the noisy appearance of the stochastic prediction, compared with the deterministic one, is still visible, yet with 1,000 channels, the stochastic and the deterministic predictions become almost superimposable (Fig 3A,C). This kind of simulation can be conveniently used to verify the accuracy of programs used, for example, to perform non-stationary noise analysis.

VII. EXPLORING THE 2-STATE MODEL WITH MARKOVEDITOR STEADY-STATE PROPERTIES

For the determination of steady-state properties, we have to specify the voltage-range over which to perform the calculations. These are inserted in the `General Settings` (see Tutorial 3 for a more exhaustive description of the `General Settings`). For example, we can impose the voltage range over which to calculate the steady-state properties to `VLeft = -100 mV`, `VRight = 100 mV`. As explained in the following, `MarkovEditor` can visualize the steady-state or time-dependent occupation probability of up to 4 different states. The states to visualize are defined by the

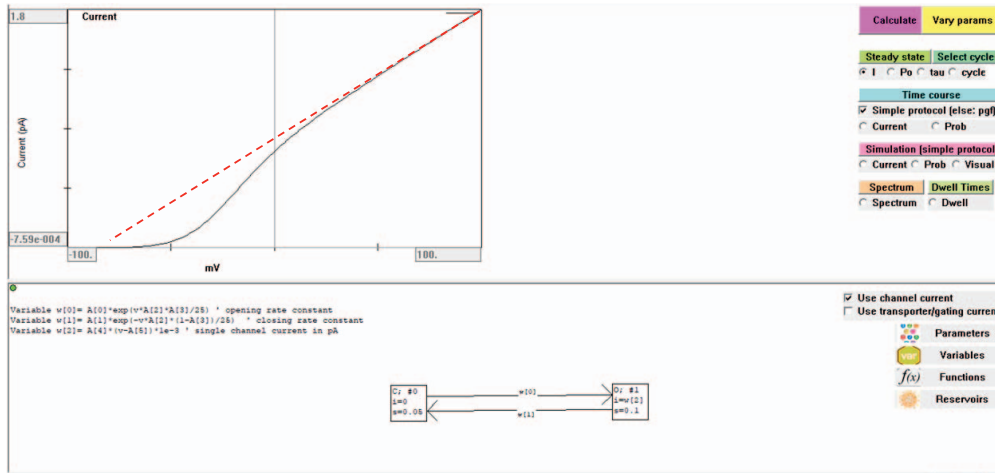
`Probability Code` variables of this dialog (`Prob 1`, `Prob 2`, `Prob 3`, `Prob 4`), which are set to states 0, 1, 2, and 3 by default but can be changed to any value, in particular for models with more than 4 states.

Now, selecting the `I` radio button under the `Steady state` tab and then clicking on the `Calculate` button will generate the graph illustrated in Figure 4A, which shows the net steady-state ion current predicted by the model. As usual, the graph offers several display options regarding the scaling of the axis and data can be easily exported, as described in Tutorial 5. The net steady-state ionic current is calculated as the sum

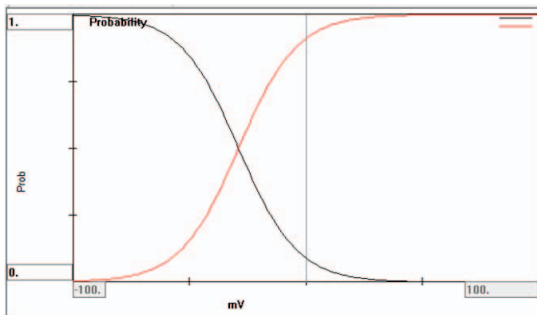
$$I_{\text{net}} = \sum_i p_i c_i \quad (24)$$

where p_i is the (steady-state) occupation probability of state i and c_i is the current value of state i . Note that for the deterministic predictions of channel properties, such as the steady-state ion current discussed here, the predictions for a single channel are calculated. The number of channels defined in the settings is not taken into consideration. The number of channels is considered only for stochastic simulations (see the previous discussion). For the 2-state potassium channel model here, the current of the fully activated channel follows a straight line for voltages more positive than +50 mV, as indicated by the dashed red line in Figure 4A. At more negative voltages, the current becomes progressively smaller, reflecting the reduced open probability. This is more evident in Figure 4B, which shows the voltage-dependent steady-state occupation probability of the closed state (in black) and the open state (in red), respectively. This graph is selected by clicking on the `Po` radio button. The Boltzmann distributions describing the occupation of the open and closed state, respectively, are nicely visible. Remaining in the `Steady state` tab, and clicking on the `tau` radio button shows, on a logarithmic scale, the voltage dependence of the relaxation time constant (Fig 4C), in full agreement with Eq.

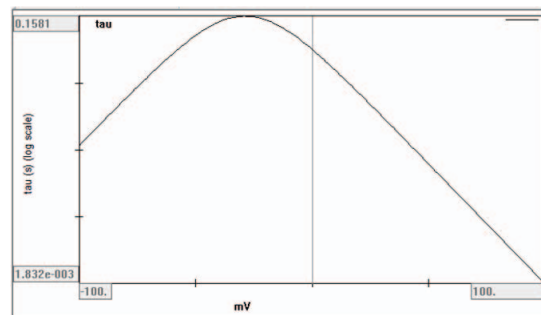
A Steady state current



B Probability



C Time constant



D Vary Params

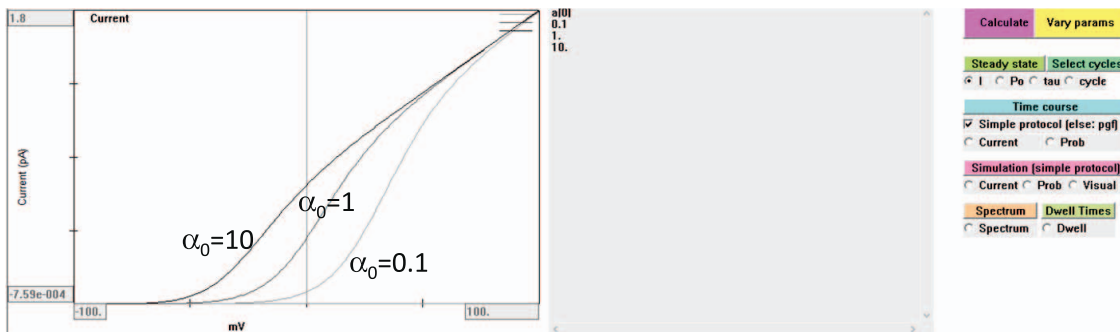


Fig 4. Steady-state predictions of the 2-state model. Panel (A) shows the current–voltage relationship (I to V curve). The dashed red line indicates the corresponding IV of a fully open channel. (B) The steady-state probabilities of the closed and open states are shown in black and red, respectively. (C) The relaxation time constant in the voltage range between -100 and 100 mV is illustrated. (D) The results of varying parameter $a[0]$ (values 0.1, 1, 10) on the steady-state IV are shown.

22. The `cycle` button applies only to models with loops and will be discussed in the following in the context of models that aim to simulate transporters.

VIII. EXPLORING THE PARAMETER SPACE WITH VARY PARAMS

The predictions of any Markov model depend on the topology of the model (not discussed here) and on the rate constants between states. To explore the behavior of the model in a certain parameter space, MarkovEditor offers the possibility to vary, in a systematic manner, one or more parameters within a certain range of values. The parameters to vary and the range over which to vary them are defined in the dialog window `Settings->Edit vary which params`. As a first example we will vary the opening rate constant at 0 mV, i.e., α_0 , in the range between 0.1 and 10, in 3 steps in a logarithmic manner, as detailed in Tutorial 6. Before initiating the exploration, we select the `I` radio button (i.e., to select `Current` to be calculated) in the `Steady state` tab and then click on the `Vary params` button. The resulting graph shows, superimposed with different gray-scales, the `I` to `V` plots for the 3 different values of the opening rate constant (indicated explicitly in a separate text box in the plot window), as shown in Figure 4D. Clicking on the `Po` radio button, results in the display of the corresponding occupation probabilities, nicely illustrating that the voltage of half-maximal activation depends on the rate constants in an exponential manner (not depicted). Similarly instructive is the illustration of the dependence of the relaxation constant on the opening rate constant (not depicted).

Another important parameter to explore is the apparent gating valence encoded by in parameter $a[2]$. For example, setting the range between 1 and 4, in steps of 0.5, nicely illustrates the dependence of the steepness of the $p_{\text{open}}(V)$ curve on the gating valence (not depicted).

IV. EXPLORING THE 2-STATE MODEL WITH MARKOVEDITOR: THE POWER SPECTRUM

The noise associated with the random fluctuations of the channel between open and closed states contains useful information (16). This information can be extracted by measuring and expressing the noise in terms of the power spectrum, as explained in detail in (17, 18). In MarkovEditor, the power spectrum can be calculated by choosing the respective radio button. Explicit formulas for the power spectrum are shown in a text window. The spectrum will be calculated for different voltages, as defined by the first segment of the simple pulse protocol in the general settings dialog. For example, setting

```
V / cl = -60
delta V / cl = 0
NPulses = 5
```

spectra will be calculated for -60 , -40 , -20 , 0 , and 20 mV. The 2-state model shows a typical single Lorentzian dependence on the frequency (not depicted). The cut-off frequency of the spectrum corresponds to the inverse time constant of the macroscopic relaxation. Note that the spectra calculated by MarkovEditor do not take into account the sigma values associated with the single-channel currents.

X. SINGLE-CHANNEL BEHAVIOR IN MORE DETAIL: THE DWELL-TIME DISTRIBUTIONS AND THE SIMPLEST LIGAND ACTIVATED CHANNEL

A standard analysis of single-channel recordings consists in the construction of the distributions of the dwell times in the various conductance states. The dwell-time distributions are then fitted with the sum of exponential functions. The number of exponential components needed to satisfactorily describe the distribution provides the number of states underlying the respective conductance state. For example, a single exponential distribution is indicative of a single state, a double exponen-

tial distribution indicates 2 states with the same conductance level (10). To illustrate this behavior, we will create a 3-state model, with 2 closed states and 1 open state. To render the model even more related to real life, we will interpret it in terms of a ligand activated channel, as illustrated in the following scheme:



Ligand L binds to the unliganded state U with rate constant $\lambda[L]$, where $[L]$ is the ligand concentration and dissociates from bound state B with rate constant μ . The bound state opens with rate constant α and the open state O closes with rate constant β . The model is entered in MarkovEditor as explained in Tutorial 7. To become acquainted with the model, we will first explore its macroscopic steady-state and kinetic properties. The ligand concentration $[L]$ is encoded in the independent variable c , playing an equivalent role as the voltage in voltage-gated channels. Having defined the range of $[L]$ in the general settings, as described in Tutorial 7, we can now calculate the dose-response behavior by using the Steady State tab and responses to concentrations steps by using the Time Course tab. Note that the maximal open probability reaches only 50% at saturating ligand concentration.

We next simulate single-channel behavior in steady state at a fixed ligand concentration, for example a low concentration of 0.1 mM. To this end, we set all concentrations of the simple stimulation protocol (see Tutorial 3) to the same value 0.1, select 1 pulse, and a sample time of 1 ms. To achieve a long simulation time of 100,000 ms, we set the duration of segment 1 to 100,000 (this field is denoted τ_1 (ms)) in the General Settings dialog. (The corresponding settings file `LigandGatedDwellTimeDistribution.set` can be found on <https://github.com/mikpusch/MarkovEditor.git>). Now selecting the `Current` radio button in the Simulation tab and clicking on `Calculate` will produce a simulated single-channel trace, which should show typical bursts of openings, separated by long shut intervals,

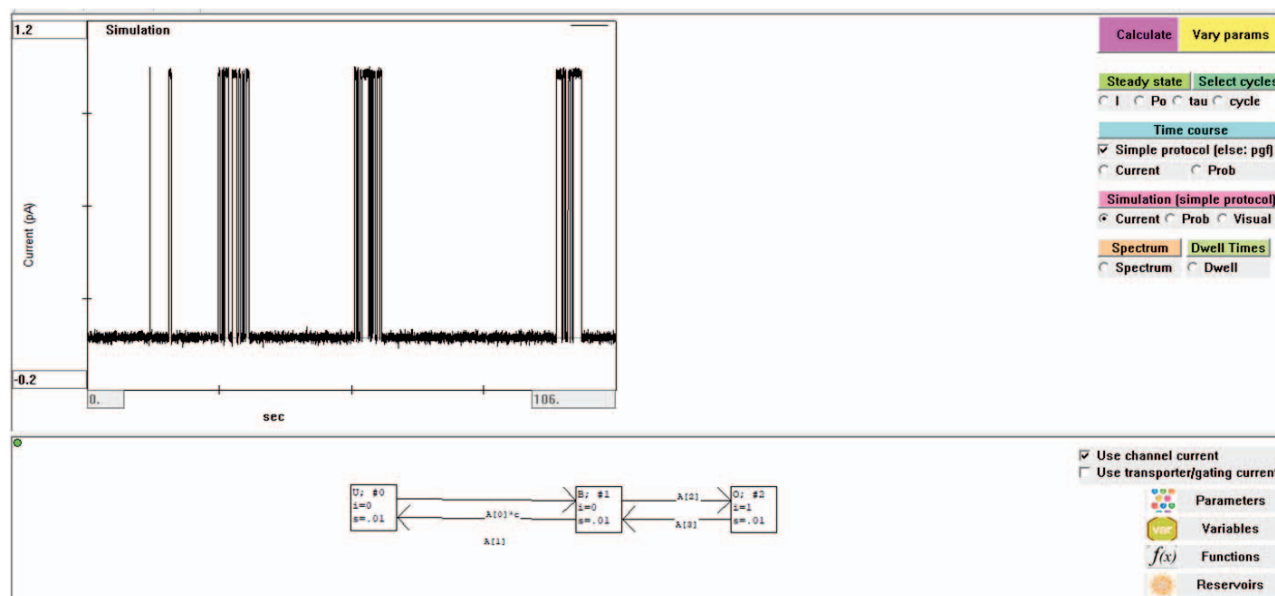
as illustrated in Figure 5A. Indeed, such bursts are encountered frequently in real single-channel recordings (11). We do not attempt to define precisely the term *burst* here but will use this example to illustrate the concept of dwell-time distributions.

Selecting the tab Dwell Times and clicking on `Calculate` will invoke the calculation of theoretic steady-state dwell-time distributions of the closed states and of the open states, respectively. These will be calculated at different concentrations or voltages, as defined by the first segment of the simple pulse protocol in the general settings dialog. For example, setting

```
V / cl = 0.1
delta V / cl = 0.9
NPulses = 2
```

dwell-time histograms will be calculated for $c = 0.1$ and for $c = 1$, as illustrated in Figure 5B. (The corresponding settings file `LigandGatedDwellTimeDistribution.set` can be found on <https://github.com/mikpusch/MarkovEditor.git>.) The cumulative distributions, $P_{\text{cum}}(t)$, provide the probability that a dwell time is longer than time t . By definition, $P_{\text{cum}}(0) = 1$ and $P_{\text{cum}}(t)$ decreases monotonically for longer times. The cumulative dwell-time distribution can be used to calculate the probability that a dwell time lies in a certain time range $[t, t+\Delta t]$ by the formula $\text{Prob}(\text{duration of event in range } [t, t+\Delta t]) = P_{\text{cum}}(t) - P_{\text{cum}}(t+\Delta t)$, which is the basis for fitting dwell-time histograms, as shown in Figure 1C. In MarkovEditor, the text window in the top middle shows the analytic expressions for the dwell-time distributions. Note that the dwell-time distribution of the open state is a single exponential (with time constant $1/\beta$), whereas the closed time distributions are double exponential, with time constants (and coefficients) that depend on the remaining rate constants and the ligand concentration. Note that the theoretic dwell-time distributions assume infinite time resolution, i.e., that all, even the shortest events are detected. In reality, often the missed events problem is far

A Bursts of a single channel



B Dwell time distributions

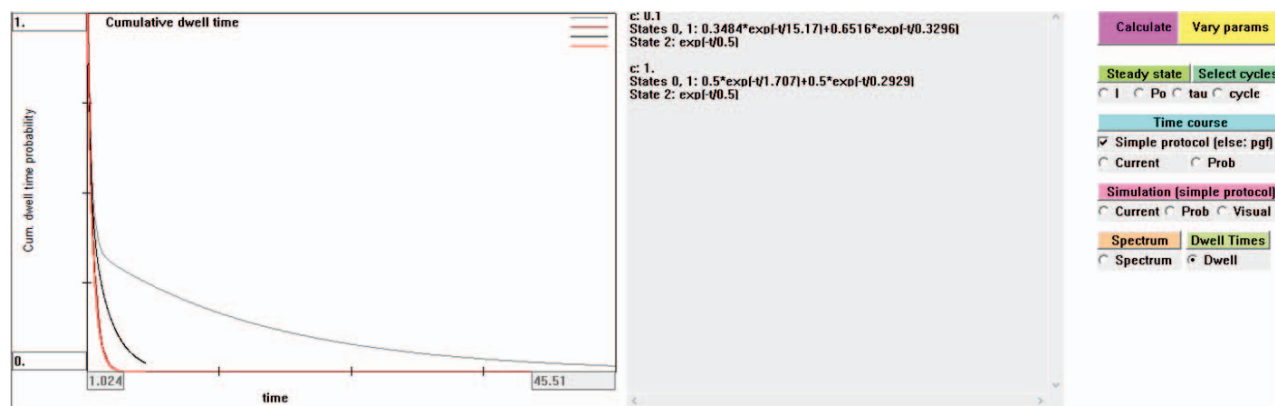


Fig 5. Ligand gated channel and dwell-time distribution. (A) A single-channel simulation of a simplified 3-state model for a ligand gated ion channel at a low ligand concentration (0.01 mM) is presented. The channel can be unbound (state U), bound (state B), and open (state O), as depicted in the lower panel. Bursts define ligand bound states during which the channel fluctuates between open and closed states. In (B) the cumulative dwell-time distributions of the 2 conductance levels (closed: black curve, representing states U and B ; open: red curve, representing state O) are shown for 2 different concentrations, as defined in the general settings (see main text). The text window provides the analytic formula of the corresponding distributions. See (11, 19, 20) for details on single-channel analysis.

from being negligible. See (19–22) for more details on single-channel analysis.

XI. A COMPLEX MODEL OF A VOLTAGE-GATED SODIUM CHANNEL: IONIC AND GATING CURRENTS

To show the capability of MarkovEditor to deal with realistic models, we will illustrate the behavior of a model of voltage-gated Na⁺ channels described by Patlak (23). At the same time, this section will serve to introduce the possibility to enter, share, and edit models by using a text-based interface. Gating of voltage-dependent Na⁺ channels involves (at least), 2 processes: activation and inactivation, leading to transient activation of Na⁺ currents upon voltage steps. In the classical Hodgkin–Huxley model, full activity is achieved by the simultaneous activation of 3 m gates, whereas inactivation is modeled by a single h gate, leading to a rather complicated model with several closed and inactivated states. For a more detailed introduction the reader is referred to (23, 24). In particular, the model we will consider is Model 7 of (23), which is inserted into MarkovEditor, as illustrated in Tutorial 8. This should result in a model display, as shown in Figure 6A (do not forget to save the model in a file to store the work done). Before going into more detail, note that parameter $w[0]$ of the model simply serves to encode the prefactor, kT/h , used by (23) to scale all rate constants (h is the Planck constant, $h = 6.63 \times 10^{-34}$ Js).

This model harbors a novel feature not discussed so far: functions. Functions are not strictly necessary, but they make life easier in certain cases. Functions conceptually differ from variables in the following way: variables are evaluated exactly once (and in order from $w[0]$, $w[1]$, and $w[2]$) when transition rates and state currents need to be calculated. On the other hand, functions are evaluated only when explicitly called within variable or state current expressions or from other functions and can be called multiple times (note that nonterminating

recursive function calls will result in program block).

The function `func[0]` in the model has been introduced to implement a restriction, proposed by Patlak (23), on the maximum value of rate constants to avoid unphysically large rate constants at extreme voltages caused by the exponential voltage dependence of the expressions for the various rate constants ($w[1]$ through $w[8]$). Slightly differently from the original Hodgkin and Huxley equations, Patlak used the expression

$$\frac{1}{\text{effective rate}} = \frac{1}{\text{calculated rate}} + \frac{1}{\text{maximum rate}} \quad (26)$$

that is implemented in

$$\text{func}[0](x) = \frac{x * a[13]}{x + a[13]} \quad (27)$$

which returns the effective rate, given the calculated rate x , and the maximum rate as set in parameter $a[13]$ (set to 20,000 s⁻¹ in the model). As can be seen in the model definition (Fig 6A and Tutorial 8), `func[0]` is applied to every single rate constant connecting the various states. This example highlights the advantage of using a reusable function in simplifying complex expressions, and it will be used in the following for the prediction of gating currents.

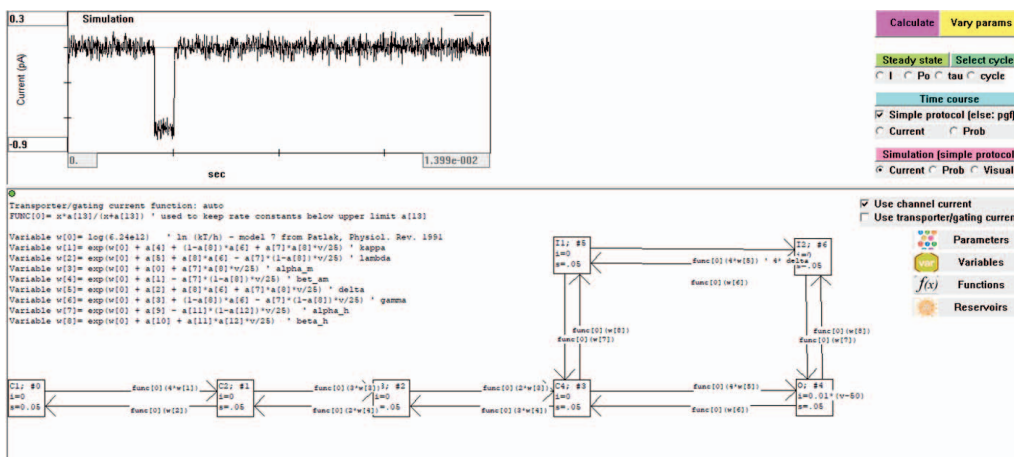
Similar to the 2-state model described in the first paragraphs, the open channel current is given by

$$i(V) = 0.01 * (V - 50) \quad (28)$$

to emulate a single-channel conductance of 0.01 nS (10 pS) and a positive reversal potential, leading to excitatory inward currents at physiologic voltages. Predictions of macroscopic and single currents upon typical voltage protocols are shown in Figure 6B,C.

In addition to the ionic currents, MarkovEditor provides the possibility to simulate so-called gating currents without any further modification of the model. Gating currents (25) arise from the movement of charges within the membrane upon changes of the membrane

A A voltage-gated sodium channel



potential. They are of capacitive nature (i.e., transient). For voltage-gated cation channels, the major part of the gating currents is mediated by the movement of the charged S4 segments (25), which leads to channel opening. In fact, the voltage dependence of the rate constants arises directly from these charge movements. Each time a voltage sensor moves outward, a tiny shotlike outward current event occurs, whose charge (i.e., time integral over the current) is equal to the effective charge movement. When the voltage sensor moves back inward, a similar inward “shot” current event is generated. On the other hand, these charge movements are the basis of the exponential voltage dependence of the rate constants (see Fig 2C). With these assumptions, the average gating current can be calculated using the rather complicated expression

$$I_{\text{gating}} = q_e \sum_i p_i \left(\sum_{j \neq i} \text{rate constant}(i \rightarrow j) z_{ij} \right) \quad (29)$$

where, as in Eqs. 16–18, z_{ij} is the gating valence conferring the voltage dependence to the transitions between states i and j ($z_{ij} = -z_{ji}$), and p_i is the probability to reside in state i . The concepts underlying the considerations leading to Eq. 29 are beautifully described in (25). Fortunately, MarkovEditor determines in a completely automatic manner the gating valences and all other parameters needed (see section XIX), allowing a straightforward prediction of gating currents.

Just 2 simple steps are needed to instruct MarkovEditor to calculate gating currents (instead of the standard ionic currents):

First, we have to check the checkbox `Use transporter/gating current` and uncheck the checkbox `Use channel current`.

Second, we have to insert the string `auto` as the `Transporter/gating current function` meaning that gating currents are automatically determined by using Eq. 29.

Alternatively, we could insert manually any expression for the `Transporter/gating current function`. This alternative mode

of inserting the gating current function can be useful to explore any specific property of a model and is explained in Tutorial 9.

Macroscopic gating currents for the Patlak Na^+ channel model are shown in Figure 6D, illustrating typical features, such as a rising phase at certain voltages. This feature differs from the predictions of the original Hodgkin–Huxley model, for which gating currents should be a decaying exponential function (23). Another feature correctly reproduced by the model of Patlak is charge immobilization, which is visible in the asymmetry between on- and off-gating currents (25). To better understand the nature of gating currents, it is also instructive to simulate them at the stochastic level, as illustrated in Figure 6E. Each time the channel undergoes a transition, a spikelike gating current, which cannot be resolved in normal patch-clamp measurements, is generated. Analysis of the nonstationary noise associated with gating currents has been used by Conti and Stühmer (26) to obtain direct experimental evidence for the quantal characteristic of gating currents.

XII. VARIATION OF A PARAMETER: INSIGHT INTO POTENTIAL DISEASE MECHANISMS

Voltage-gated sodium channels play a role in most excitable cells (neurons, skeletal, muscle, heart, and endocrine cells) and defects in the respective encoding genes lead to a plethora of human genetic diseases (27, 28). A rather frequent phenotype of disease causing mutations is the appearance of so-called “persistent” currents, or more generally, defects that render the inactivation process less efficient; see (29–31). For example, the mutation T1313M in the muscle Nav1.4 channel causes paramyotonia congenita and is associated with significant persistent currents, shifted voltage dependence of inactivation, and faster recovery from inactivation (29). MarkovEditor allows us to develop hypotheses about the molecular mechanisms underlying such a functional defect, as illustrated in Figure 7. We concen-

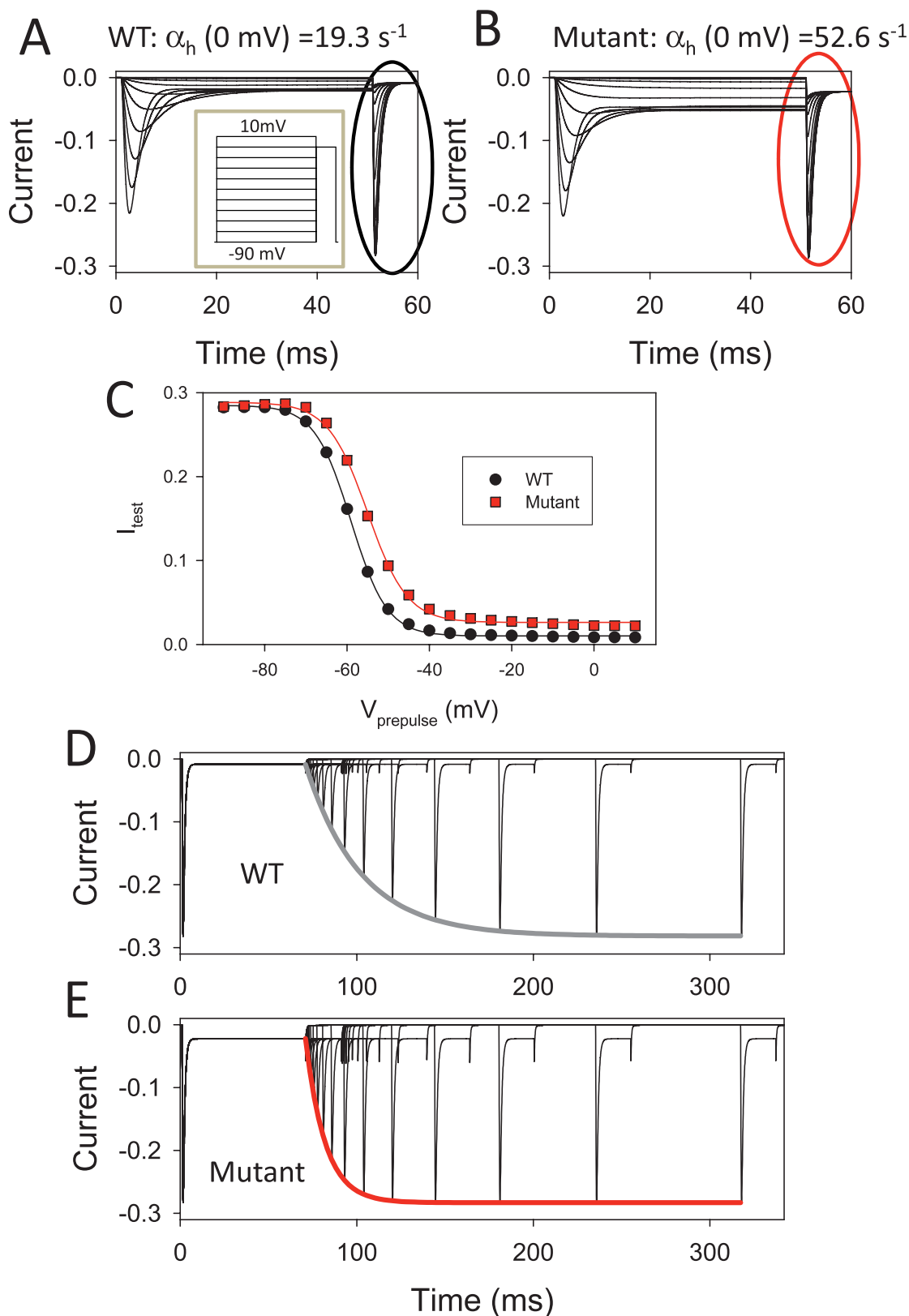


Fig 7. Simulation of a disease phenotype – disruption of fast inactivation in a mutation of the Na^+ channel causing paramyotonia congenita. Panels (A and B) show predictions of macroscopic currents of the WT Patlak model (i.e., with $a[9] = -26.5$, resulting in $w[7] = 19.3 \text{ s}^{-1}$ at 0 mV) or a mutant model (i.e., with $a[9] = -25.5$, resulting in $w[7] = 52.6 \text{ s}^{-1}$ at 0 mV) by using the voltage clamp protocol shown in the inset in (A). The steady-state inactivation protocol is also contained in the pgf `Pulses.pgff`, which can be downloaded from <https://github.com/mikpusch/MarkovEditor.git>. The ellipses in (A and B) highlight the test currents elicited by a 10-mV

trate on the single parameter α_{h0} , which is the rate constant important for recovery from inactivation. The value of α_{h0} is determined by parameter $a[9]$ and calculated in variable $w[7]$ in the model (see Tutorial 8). For wild-type (WT), $a[9] = -26.5$, which via variable $w[7] = \exp(w[0] + a[9] - a[11] * (1 - a[12]) * v / 25)$ results in α_{h0} (i.e., at 0 mV) $\sim 19.3 \text{ s}^{-1}$. To increase α_{h0} e-fold, i.e., by a factor of 2.71, we set $a[9] = -25.5$, resulting in $\alpha_{h0} \sim 52.6 \text{ s}^{-1}$. This simple maneuver leads to a number of changes. Figure 7A,B show the response of WT channels and mutated channels to a typical voltage-protocol used to measure steady-state inactivation. Clearly, the mutated channels exhibit much larger persistent currents. After the long pulses to various voltages, channel availability is measured by a final test pulse to 0 mV, and the resulting (absolute) peak values are plotted in Figure 7C as a function of the conditioning voltage. The solid lines are fits with a Boltzmann distribution. The mutant data are slightly shifted to more positive voltages. Finally, Figure 7D and E illustrate the response to a typical protocol used to measure the speed of recovery from inactivation. After a 70-ms inactivating prepulse, the membrane voltage is kept at -90 mV for increasing time, and channel availability is measured by a test pulse to 0 mV. WT channels recover in a monoexponential manner (gray line in Fig 7D) with a time constant that is 3 times slower than mutant channels (red line in Fig 7E). This is just a simple example of how MarkovEditor can be used to glean mechanistic insight into the effect of disease-causing mutations.

XIII. A SIMPLE ELECTROGENIC UNIORTER

Even though initially designed to model ion channels, MarkovEditor is well capable of

simulating even complex transporters, both at the steady-state level, and in terms of transient currents, which is relevant for electrogenic transporters. This will be illustrated here using a simple electrogenic uniporter, described by 4 states, as illustrated in Figure 8. The uniporter can expose its binding site either to the outside (upper states) or to the cytosol (lower states). The conformational change between these configurations is assumed to be intrinsically voltage dependent (indicated by the movement of the “green” negative charge in Fig 8), and translocation of the positively charged substrate confers an additional voltage dependence to the loaded transporter. Binding and release of substrate may also be voltage dependent. For example, this is the case for Na^+ binding in the Na-K-ATPase (32). This specific transporter model incorporates several features highlighted and investigated by researchers (33–35). The model can be inserted into MarkovEditor using the text-based method, as detailed in Tutorial 10. Alternatively, the model file `Uniporter.mod` can be downloaded from <https://github.com/mikpusch/MarkovEditor.git>. Regarding the equations and symbols depicted in Figure 8, the parameters of the model are used with the following conventions:

$a[0]$: δ_4 , effective valence of the charge associated with the conformational change from outside to inside, independent of substrate binding. The parameter combines both the actual charge as well as the electrical distance associated with the charge movement into a single number. In effect, for a complex protein, the simplification consists in replacing by a single effective valence the movement of diverse charges and dipole moments in the apoprotein during its structural transition. The value of $a[0]$ is

←

test pulse. The respective (absolute) peak-current values are plotted in (C) together with fits of a Boltzmann function (lines). (D and E) Results for a typical experiment were aimed at measuring the speed of recovery from inactivation. After a long (70-ms) depolarization to inactivate most channels, the membrane potential is returned to -90 mV for increasing duration, followed by a test pulse to 0 mV. The recovery protocol is also contained in the pgf `Pulses.pgf`, which can be downloaded from <https://github.com/mikpusch/MarkovEditor.git>. The gray and red lines in panels (D and E) are fits of single exponential functions to the peak currents with $\tau = 31.1 \text{ ms}$ (WT), and $\tau = 11.1 \text{ ms}$ (mutant), respectively.

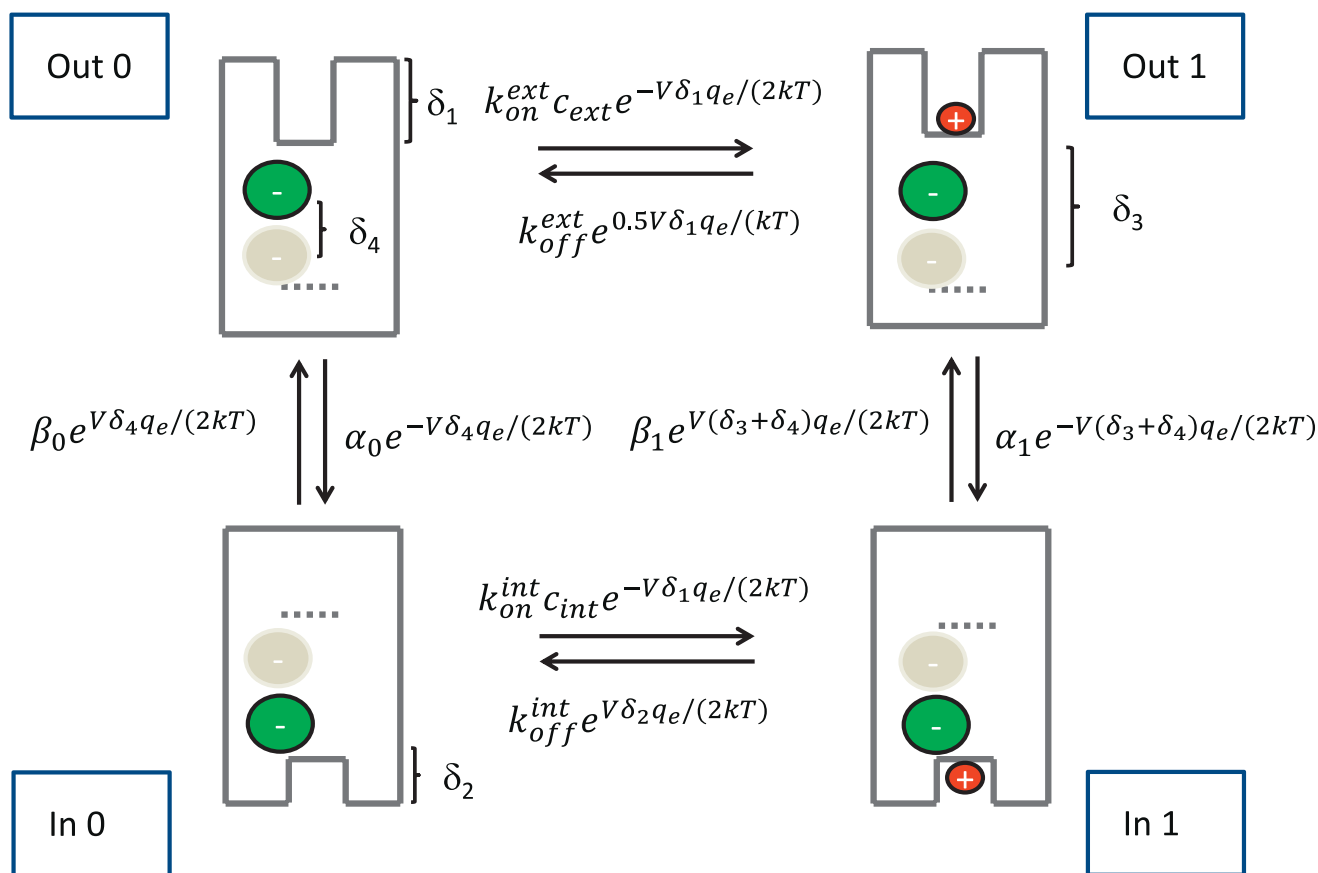


Fig 8. A 4-state electrogenic uniporter. The outwardly oriented empty transporter (state Out 0) binds the positively charged substrate (red circle) from the outside, with a voltage dependence given by the electrical distance δ_1 (state Out 1). The conformational change from outwardly oriented binding site (upper states) to the inwardly oriented site (state In 1) is associated with an intrinsic voltage dependence (green sphere, electrical distance: δ_4 ; see main text for the simplification underlying this concept of intrinsic charge). For the loaded transporter, the transfer of the charged substrate adds to the voltage dependence, (electrical distance: δ_3). Binding and release of substrate from the inside is associated with the electrical distance δ_2 (state In 0). The expression of the rate constants explicitly shows the exponential voltage dependence. Note that for simplicity, we impose symmetrical electrical barriers for ligand binding and structural transitions resulting in the “.../(2 kT)” expression in all exponentials.

negative to emulate a negative intrinsic charge!

- a[1]: δ_1 , electrical distance of the binding site exposed to the outside.
- a[2]: δ_3 , electrical distance associated with moving of substrate from outer open state to inner open state.
- 1-a[1] -a[2]: δ_2 , electrical distance of the binding site exposed to the inside.
- a[4]: α_0 , rate constant (at 0 voltage) of conformational change from outside exposing to inside exposing binding site of empty transporter.
- a[6]: α_1 , rate constant (at 0 voltage) of conformational change from outside exposing

ing to inside exposing binding site of loaded transporter.

- a[7]: β_1 , rate constant (at 0 voltage) of conformational change from inside exposing to outside exposing binding site of loaded transporter.
- a[8]: $k_{\text{off}}^{\text{int}} = k_{\text{off}}^{\text{ext}}$, unbinding rate constant of substrate (at 0 voltage) of substrate to inside or outside, assumed to be equal.
- a[9]: $k_{\text{on}}^{\text{int}} = k_{\text{on}}^{\text{ext}}$, association rate constant of substrate (at 0 voltage) of substrate from inside or outside, assumed to be equal.
- a[32]: c_{ext} , extracellular substrate concentration.
- a[33]: c_{int} , intracellular substrate concentration.

Note that for simplicity (to reduce the number of parameters), the affinity of the outwardly oriented binding site is assumed to be identical to that of the inwardly oriented binding site.

An extremely important aspect regarding models of transporters, or more generally models involving loops or cycles, is the second law of thermodynamics and the impossibility to construct a *perpetuum mobile*. For example, for the uniporter model the following sequence of state occupancies

Out 0 → Out 1 → In 1 → In 0 → Out 0

would represent a clockwise cycle of transport corresponding to an inward transport of a substrate molecule. However, to achieve a completed inward transport cycle, the transporter may go back and forth between states several times. Therefore, also the following sequence of state occupancies would be a clockwise cycle associated with the inward transport of a substrate molecule:

Out 0 → Out 1 → In 1 → Out 1 → In 1 → In 0 → In 1 → In 0 → Out 0.

By analogy, out of many possible cycles, the inverted sequence of the previous cycle

Out 0 → In 0 → In 1 → In 0 → In 1 → Out 1 → In 1 → Out 1 → Out 0

represents an anticlockwise cycle, corresponding to the outward transport of a substrate molecule. To be physically realistic, Markov models have to obey the second law of thermodynamics. This implies that in conditions of thermodynamic equilibrium, no net cycling can occur for any cycle of the Markov scheme. This means that, on average, the number of cycles completed in the clockwise direction has to be identical to the number of cycles completed in anticlockwise direction (36). Otherwise, the transporter would be able to accumulate substrate on one side of the membrane without external energy input. This principle is also called *microscopic reversibility* and applies only to equilibrium conditions. In case of the electrogenic uniporter discussed here, equilibrium conditions are zero trans-

membrane potential and equal substrate concentrations on the inside and on the outside. Fortunately, this constraint can be easily incorporated into the model because it is equivalent to the requirement that, for each cycle,

$$\prod_{\text{clockwise}} \text{rate constants} = \prod_{\text{anticlockwise}} \text{rate constants} \quad (30)$$

i.e., that the product of rate constants in the clockwise direction of each cycle is equal to the product calculated in the anticlockwise direction (36). In equilibrium conditions, i.e., $V=0$, $C_{\text{ext}}=C_{\text{int}}$, for the uniporter model, the previously mentioned condition translates into

$$k_{\text{on}}^{\text{ext}} \alpha_1 k_{\text{off}}^{\text{int}} \beta_0 = k_{\text{on}}^{\text{int}} \beta_1 k_{\text{off}}^{\text{ext}} \alpha_0 \quad (31)$$

Because we assumed the binding or unbinding properties to be equal for both inward- and outward-facing configurations of the transporter, the constraint can be simplified and reformulated as

$$\beta_0 = \frac{\alpha_0 \beta_1}{\alpha_1} \quad (32)$$

This has been incorporated in the model in that variable $w[1]$ is calculated as

$$w[1] = a[4] * a[7] / a[6] \quad (33)$$

which is then used to calculate β_0 .

After these lengthy, but important considerations we are almost ready for the predictions of the uniporter model. To calculate the current generated by the model, we have to check the checkbox `Use transporter/gating current` and uncheck the checkbox `Use channel current`, and we have to insert a valid `Transporter/gating current function`. As for the gating currents of the voltage-gated sodium channel model, the easiest choice for this is `auto`, which derives the charge translocation steps from the voltage dependence of the rate constants.

Importantly, it is possible to insert any syntactically valid function as the `Transporter/gating current function`,

allowing the analysis of every aspect of the model.

For example, for a single-cycle model as the uniporter model, the net cycling frequency is proportional to the net transport activity, which can be expressed as

$$p[2] * w[5] - p[0] * w[7] \quad (34)$$

Here, $p[2]$ is the (time-dependent) occupation probability of state 2, and $w[5]$ the rate constant of transitions from state 2 (outside oriented, substrate bound) to state 0 (outside oriented, no substrate bound, “apo”). Thus, the product $p[2] * w[5]$ is the effective rate of transitions from state 2 to state 0. Similarly, the product $p[0] * w[7]$ is the effective rate of transitions from state 0 to state 2. For any cyclic scheme, the difference of such rates of neighboring states provides the net cycling frequency in steady-state conditions (36). Thus, Eq. 34 can be used alternatively as the `Transporter/gating current function` for the purpose of steady-state calculations. However, with this equation, not all the transitions contributing to the transient currents are correctly taken into account resulting in errors in the calculation of transient (or presteady-state) currents, as well as the power spectrum. Therefore, for the electrogenic uniporter discussed here, we will stick to the choice of `auto` for the `Transporter/gating current function`.

In addition to microscopic reversibility, care has to be taken in assigning the correct voltage dependence to each rate constant to maintain a correct treatment of net inward versus outward charge movement. For the electrogenic uniporter model, the formal correctness of the equations can be checked by assuring that the calculated reversal potential corresponds to the Nernst potential (6). At the Nernst potential, outwardly directed transport cycles occur at the same (average) frequency of inwardly directed transport cycles. An uphill transport of the substrate against the electrochemical equilibrium in the absence of an external energy input would violate the thermodynamic laws. The Nernst potential is given by

$$E_{\text{rev}} = \frac{kT}{q_e} \ln \left(\frac{c_{\text{ext}}}{c_{\text{int}}} \right) \approx 25 \text{ mV} \ln \left(\frac{c_{\text{ext}}}{c_{\text{int}}} \right) \quad (35)$$

(at room temperature $kT/q_e \sim 25 \text{ mV}$). We will perform this test in a first exercise. We assign

$$a[32] = 10 = c_{\text{ext}} \text{ and } a[33] = 1 = c_{\text{int}}.$$

Inserting these 2 concentrations into Eq. 35 yields a theoretic reversal potential of $E_{\text{rev}} = 25 \text{ mV} \times \ln(10) = 57.6 \text{ mV}$. To simulate the steady-state IV relationship, we check the `I` radio button in the Steady State tab and click on the `Calculate` button, which should result in the display of the steady-state IV as shown in Figure 9A. Exporting the data to a spreadsheet (via right-clicking on the graph) allows to verify that the simulated data closely follow the predicted reversal potential.

The `Vary params` feature allows us to investigate the dependence of transport on intracellular and extracellular substrate concentration, as well as on all other parameters. As an example, Figure 9B illustrates the effect of varying the intrinsic charge associated to transport function (δ_4 in Fig 8).

XIV. PRESTEADY-STATE CURRENTS OF THE UNIPORTER

Upon abrupt changes of the membrane potential, the initial relaxation of the transporter toward a new steady-state condition, as exemplified in Eq. 11 for the 2-state model, results in transient or presteady-state currents, before reaching the steady transport level. In this case, we use `auto` as the `Transporter/gating current function` and the current relaxations faithfully reflect the predicted transient (and steady-state) currents of the model, as all transitions are taken into account. These transient currents provide important information on the transport mechanism, but they are often difficult to measure because they are partially masked by the capacitive currents associated with the charging of the cell membrane capacitance. In specific cases, this problem can be partially circumvented by comparing the transient currents in the presence and in the absence

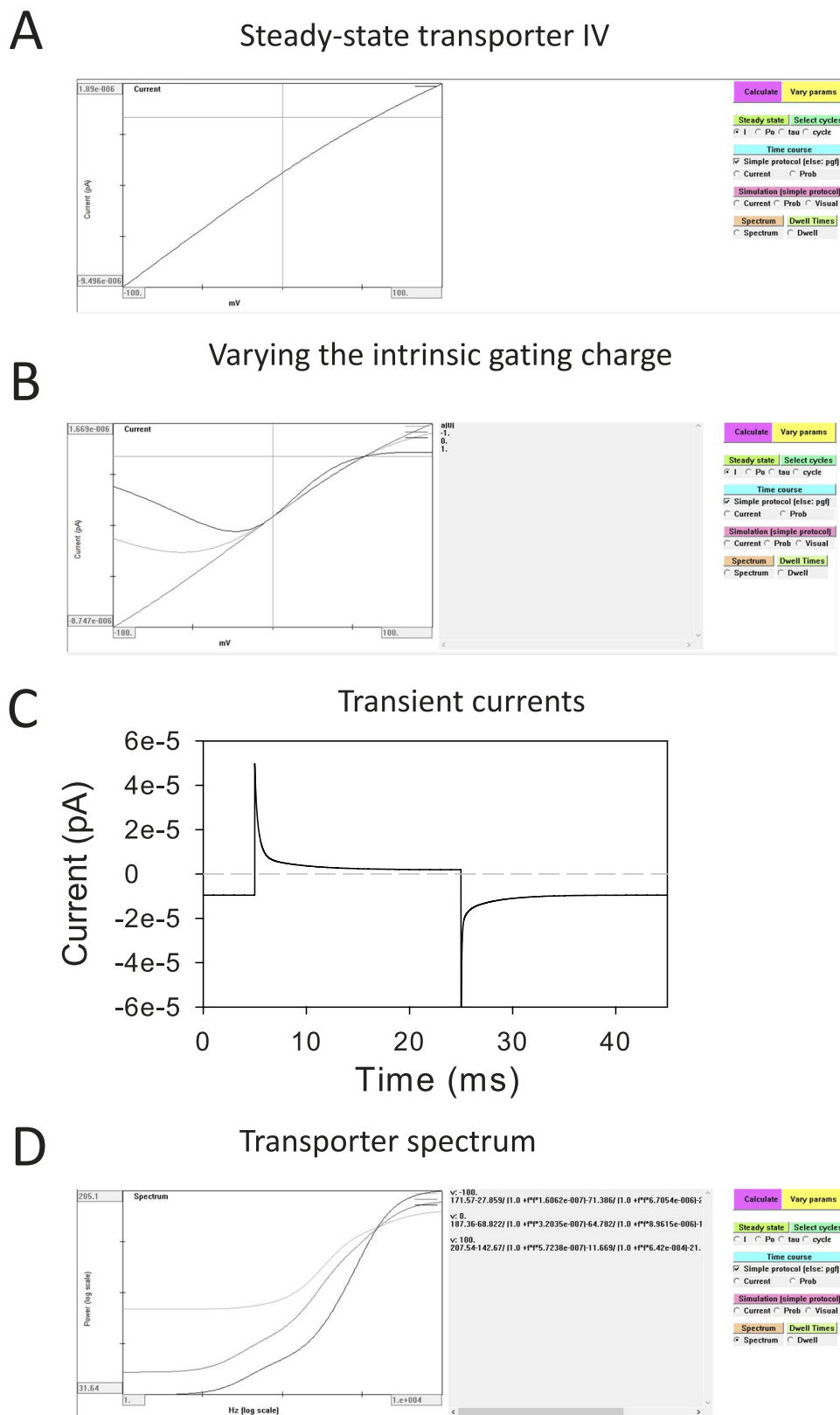


Fig 9. Predictions of the uniporter. (A) Steady-state IV calculated between -100 and $+100$ mV with extracellular concentration of the substrate, $c_{\text{ext}} = 10$ mM, intracellular concentration, $c_{\text{int}} = 1$ mM. (B) The effect on the steady-state IV of varying the intrinsic gating charge (green sphere in Fig 8) between -1 and $+1$ is encoded by the parameter $A[0]$. (C) Transient ensemble currents were calculated for a step from a holding voltage of -100 to 100 mV (20 ms), followed by repolarization to -100 mV. (D) Power spectra of the transporter at -100 , 0 , and $+100$ mV and with $c_{\text{ext}} = 10$ mM, $c_{\text{int}} = 1$ mM both graphically (on double logarithmic scale), as well as explicit formula (in gray textbox).

of the substrate (37). For the 4-state uniporter investigated here, typical ideal transient currents are illustrated in Figure 9C.

XV. THE TRANSPORTER SPECTRUM

In any condition, even at thermodynamic equilibrium, the electrogenic stochastic transitions of the transporter, which might be either substrate binding or unbinding events, or conformational changes, are associated with tiny spikes of the electric current, as already discussed in the framework of the gating currents of the sodium channel. For a given Markov model, the power spectrum of the noise generated by these transitions can be predicted in an explicit manner (34, 35). In principle, the power spectrum could provide important information on the underlying transport mechanism, but, unfortunately, experimentally the power spectrum is difficult to measure in real life. In MarkovEditor, the spectrum will be calculated for different voltages, as defined by the first segment of the simple pulse protocol in the general settings dialog. For example, setting

```
V / c1 = -100
delta V / c1 = 100
NPulses = 3
```

spectra will be calculated for -100 , 0 , and 100 mV. MarkovEditor visualizes the power spectra at these voltages, both graphically as well as in analytic formulas. The typical spectrum of a transporter is qualitatively different from that of a channel because of the shot noise properties of the electrical events associated with transporter activity. The examples for the uniporter, shown in Figure 9D, are calculated at -100 , 0 , and 100 mV with $c_{\text{ext}} = 10$ mM, $c_{\text{int}} = 1$ mM. The spectra rise from a low-frequency limit to a high-frequency limit with 3 separate Lorentzian components. The correctness of the theoretic spectra can be verified by stochastic simulation of a large number of transporters and calculation of the power spectrum on the exported data.

XVI. CYCLING FREQUENCY OF THE UNIPORTER

For transporters, and more general, for all Markov models that contain closed loops, the frequency of clockwise and anticlockwise cycling is an interesting property. For example, as noted previously, in thermodynamic equilibrium, these 2 cycling frequencies have to be equal. For a transporter with a single cycle, as the 4-state uniporter, the difference in clockwise and anticlockwise cycling frequency determines the effective transport rate. Using the method of Hill (36), MarkovEditor is able to calculate the clockwise and anticlockwise cycling frequencies for each cycle. The cycle to be calculated has to be chosen by clicking on `Select cycles`. For the uniporter model, only a single cycle is present. After the selection, checking the radio button `cycle` and clicking on `Calculate`, will produce the clockwise (in red) and anticlockwise (in black) cycling frequencies (in units of s^{-1} ; Fig 10A). At the reversal potential, these 2 frequencies are equal. Note that for models with a large number of cycles, the algorithm used is not very efficient.

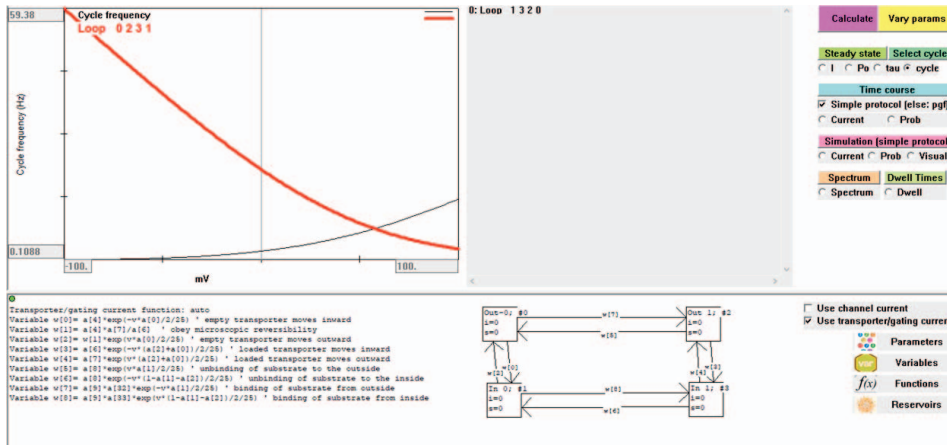
XVII. SINGLE TRANSPORTER SIMULATIONS

At present, the electrical current associated with single transporters is beyond experimental resolution. However, single-molecule fluorescence techniques have been used to follow conformational changes of certain, rather slow bacterial transporters (38). The simulation of single transporter activity can thus provide a guide to interpret single-molecule measurements. MarkovEditor can, on one hand, simulate the single transporter electrical activity, as illustrated in the section on gating currents of the voltage-dependent sodium channel. This feature will be used in XVIII section to validate the calculation of the power spectrum of transporter generated currents.

On the other hand, the following trick can be used to visualize the stochastic behavior of a single transporter molecule. To follow the transitions of a single transporter in time, we

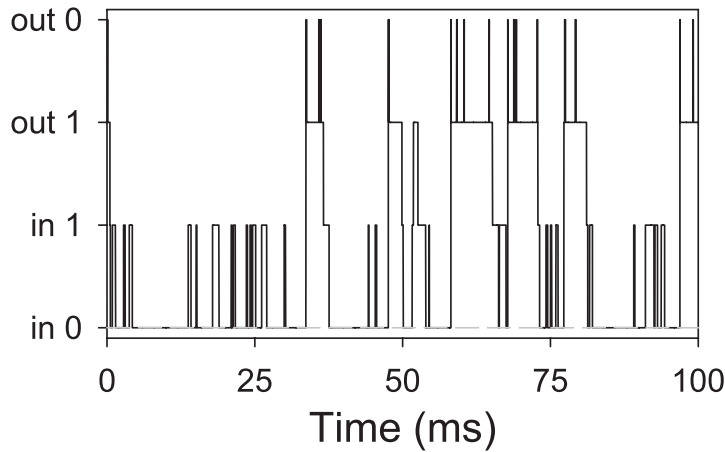
A

Cycling frequency



B

Cycling of a single transporter



C

Visual simulation of a single transporter

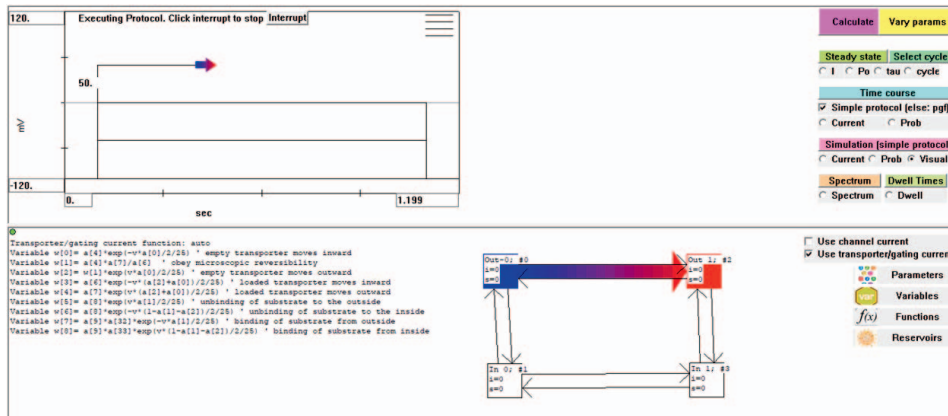


Fig 10. Cycling of the uniporter. (A) Cycling frequency of the uniporter as a function of voltage in asymmetric conditions ($c_{ext} = 10$ mM, $c_{int} = 1$ mM). The red line shows the (average) absolute frequency (in s^{-1}) of completed clockwise cycles, corresponding to inward substrate transport, whereas the black line indicates anticlockwise cycle frequency. Note that the cycling frequencies are identical at the Nernst potential of 57.6 mV, at which, consequently, no net transport occurs. (B) To follow the state sequence during the stochastic simulation, fictitious current values have been assigned to each state. With this trick, the irreversible net clockwise cycling at -100 mV and with $c_{ext} = 10$ mM, $c_{int} = 1$ mM is nicely visible at the level of a single transporter.

artificially assign a distinct current value to each state. In this way, the simulated current trace of a single transporter of the transporter will reflect the transitions between the various states. In the example illustrated in Figure 9D, we chose the following values:

3 for state `Out 0`
 2 for state `Out 1`
 1 for state `In 0`
 0 for state `In 1`

Furthermore, we uncheck the checkbox `Use transporter/gating current` and check the checkbox `Use channel current`, to visualize the fake specific-state associated ion currents. Then, assigning asymmetric ion conditions and simulating (e.g., for 100 ms), Figure 10B clearly illustrates the net clockwise cycling. The trace shows a clear asymmetry regarding the direction of time. In equilibrium conditions (e.g., at the Nernst potential), no statistical method should be able to distinguish the time-reversed signal from the ordinary signal. In this context, an instructive example is the single-channel analysis of Richard and Miller of the Torpedo chloride channel, which revealed that channel gating is not at thermodynamic equilibrium (39).

XVIII. VISUAL SIMULATION OF A SINGLE TRANSPORTER

An alternative way to explore the behavior of a single channel or transporter is provided by the visual simulation. With this feature, the time-dependent simulated stochastic behavior of a single channel, calculated according to the simple protocol defined in the General Settings, is visualized in a time-dependent manner by highlighting the actually occupied state in red and the previously occupied state in blue (see Fig 10C). Furthermore, the previously occupied state and the currently populated state are connected by a colored arrow. The frame rate at which the simulation is reproduced is defined by the `time step in visual simulation` in the General Settings. In other words, each time step of the simulation (defined by the sample time) is going to be

visualized on screen for the duration defined by the `time step in visual simulation` (the settings file `UniporterVisualSimulation.set` can be downloaded from <https://github.com/mikpusch/MarkovEditor.git>) In parallel, the graph in the upper pane shows the current time point of the simulation protocol. The currently active protocol value is shown as a number, and a small colored arrow indicates the progress through the protocol. To invoke the visual simulation, select `Visual` in the `Simulation` tab and click `Calculate`. To interrupt an ongoing visual simulation, simply click on the `Interrupt` button or click again on `Calculate`. It may happen that the colored arrow is connecting states for which no direct transition is actually permitted. This behavior is possible if, during a single sample period, more than one transition occurs. In fact, as described in section XIX, such missed events are realistically modeled in MarkovEditor. The visual simulation is not limited to transporter models but is applicable to every type of model.

XIX. METHODS

A. Method of deterministic numeric simulation

The Markov model is defined by a number of states N , connected by voltage-dependent rate constants r_{ij} for transitions from state i to state j . For deterministic simulations, the time-dependent occupation probabilities $p_i(t)$ are governed by the differential equations

$$\frac{dp_i}{dt}(t) = \sum_{i \neq j} p_j r_{ji} - p_i \sum_{i \neq j} r_{ij} = \sum_j p_j q_{ji} \quad (36)$$

defining the Q matrix given by the components q_{ij} . The program can handle up to 100 states. Stationary occupation probabilities are denoted by π_i for state i and are calculated by standard matrix inversion. For temporal analysis, the (possibly complex) eigenvalues and eigenvectors of the Q matrix in MarkovEditor are determined by using the ALGLIB C library (<http://www.alglib.net>). For nonconstant segments (i.e., ramp, sine, wave; see Tutorial 6),

numeric solution is performed by using an eighth-order Dormand–Prince integration algorithm (40). This may lead to slow execution in case of complex models.

For ion channel models, each state i is associated with a voltage-dependent current c_i . In the tool described here, an arbitrary voltage-dependent function can be assigned for the current of each state. A common simplified assumption is that the open channel current depends in a linear manner on the membrane voltage. For example, for a 50-pS channel with an assumed reversal potential of -30 mV, a suitable function to describe the open channel current is given by $0.05 \times (v + 30)$ with the implicit convention to measure voltage in millivolts and current in picoamperes.

For closed states, the current function should be 0. In addition to the current for each state, the simulation program also provides the opportunity to assign a noise level for each state (given as the standard deviation in picoamperes). This is only used for the stochastic simulation of a discrete number of channels (see the following).

Having assigned the microscopic current c_i for each state i , the predicted channel current, I_{chan} , in the deterministic mode, is given by

$$I_{\text{chan}}(t) = \sum_i p_i(t)c_i \quad (37)$$

B. Transporter and gating currents

In addition to the open channel current, c_i , transitions between states may be associated with a charge movement reflecting for example gating charge movement in voltage-gated channels or, more general, any electrogenic step in a transporter or channel. On a microscopic scale, these electrogenic steps correspond to a current spike, idealized by a delta function, whose time integral is given by the charge moved in the step. On a macroscopic, deterministic scale, the electrogenic steps produce an average, transient current I_{trans} , given by

$$I_{\text{trans}}(t) = \sum_{i,j} p_i(t)r_{ij}Q_{ij} \quad (38)$$

where Q_{ij} is the charge moved upon the transition from state i to state j .

Within MarkovEditor, there are 2 different ways to calculate I_{trans} :

- In the most general manner, it is possible to explicitly define a function, called the *Transporter/gating current function*, used to calculate I_{trans} , as illustrated for an example in the Tutorial 9.
- In most models of channels and transporters, transition rates depend exponentially on the applied voltage, with the translocated charge, Q_{ij} , determining the voltage dependence. For example, the opening and closing rate constants, α (V) and β (V), respectively, might be given by

$$\alpha(V) = \alpha_0 e^{\frac{z_\alpha V F}{RT}} \quad (39)$$

and

$$\beta(V) = \beta_0 e^{\frac{z_\beta V F}{RT}} \quad (40)$$

where α_0 and β_0 are the respective rate constants at 0 mV, z_α and z_β the respective gating valences, and F , R , T the Faraday constant, the gas constant, and the absolute temperature, respectively, with $kT/q_e \sim 25$ mV at room temperature. For such a transition, the value of the translocated charge for the opening transition is $(z_\alpha - z_\beta) \times q_e$, where q_e is the absolute charge of an electron. The charge for the closing transition is the negative value of that of the opening transition, that is $(z_\beta - z_\alpha) \times q_e$. More generally, the translocated charge of transition (i,j) at a given voltage can be determined by the logarithmic derivative with respect to voltage of the rate constants involved in the transition:

$$Q_{ij} = \left(\frac{d \ln(r_{ij})}{dV} - \frac{d \ln(r_{ji})}{dV} \right) kT \quad (41)$$

where k is Boltzmann's constant and T is assumed to be 300 K. This procedure for determining the translocated charges is selected in the simulation program by choosing `auto` as the `Transporter/gating current function` in Markov Editor (or by leaving this field blank). With

this setting, MarkovEditor uses the logarithmic derivative of the rate constants to determine the translocated charge (Eq. 41), and Eq. 38 to calculate the transporter and gating currents associated with the model. This choice is the simplest and, in most cases, an adequate mode of selection.

C. Method of stochastic simulation

So far, we have described the use of deterministic simulations of the properties of a finite number of ion channels or transporters. However, one could also use a stochastic approach (analyze the behavior of the ensemble starting from the properties of a single channel or transporter), under the assumption that they behave independently of each other. In this case, because each channel or transporter is modeled independently, the time needed for simulation is proportional to the number of channels and becomes prohibitive for a very large number of channels.

This mode of operation is useful, for example, to explore the variability of possible experimental results, if the underlying data would be described by a given Markov model. This mode also allows to test predictions of stationary and nonstationary noise analysis.

In the stochastic simulation mode of channels it is possible to include a noise level for each channel state. The noise is specified as the standard deviation of a Gaussian white noise level added on top of the current level of a channel state. This can be used for example to create realistically looking channel events, as we saw in Figure 4, or to test the influence of open channel noise on noise analysis or other types of analysis. It is also useful to test the capabilities of single-channel analysis software, in particular, regarding missed events detection. The stochastic simulation of a single transporter or channel is exact in the sense that it is independent from the sampling time selected in the sampling procedure.

At the beginning of each sweep, the holding potential determines a starting state, using a random number chosen between 0 and 1, and the stationary occupation probabilities π_i . For example, for a 2-state model with $\pi_0 = 0.3$, $\pi_1 =$

0.7, a random number <0.3 would lead to the selection of state 0 as the starting state, whereas a larger random number would select state 1. Random numbers are calculated by using the Mersenne Twister pseudorandom number generator (<http://www.math.sci.hiroshima-u.ac.jp/~m-mat/MT/MT2002/CODES/mt19937ar.c>). Once a state i has been specified, the mean sojourn time in this state is given by the inverse of the sum of all rate constants leaving that state (11):

$$\tau_i = \frac{1}{\sum_j r_{ij}} \quad (42)$$

Using a random number r in the interval $]0..1]$, a stochastic prediction of the time spent in this specific state is given by

$$T = -\ln(r) * \tau_i \quad (43)$$

If the command voltage changes to a new value at any sampling instance before reaching time T , the rate constants are recalculated and a new dwell time is computed. The approach exploits that by virtue of the digitalization and discrete sampling, the command voltage changes stepwise. The procedure to calculate a new dwell time, independent of the time already spent in a given state, is valid because of the memoryless nature of a Markov process. At the end of the dwell time, the state to which the system will jump is determined with a novel random number and using the rate constants departing from the current state as relative weights in the decision. The timing of the jump is independent from the sampling time, and it may indeed happen that the system is changing state more than once during a given sampling period, leading effectively, and in a realistic manner, to missed events in the simulation.

To simulate the transporter or gating current spikes, the charge associated with the transitions is summed during each sample period providing Q_{net} , the net charge translocated during a sampling period. Then, the current signal $Q_{\text{net}}/\Delta t$, where Δt is the sampling interval, is added to the overall current sampling output.

XX. TUTORIAL 1: INSTALLING MARKOVEDITOR ON A WINDOWS COMPUTER

MarkovEditor is specific for Windows (Microsoft Corporation, Redmond, WA) and runs on Windows XP (Microsoft) and higher (including Windows 10, Microsoft). The code is written in Microsoft Visual C++, and although it is fully compatible with VisualStudio 2019 (Microsoft), the current build is done with VisualStudio 2005, allowing execution on Windows XP, which is still in use in many less developed countries. The source code is available on request. The program should run on Windows emulators on Mac (Apple Inc., Cupertino, CA) and Linux (Linux Foundation, San Francisco, CA).

You can download the MarkovEditor master zip file from <https://github.com/mikpusch/MarkovEditor.git>. Save the program file `MarkovEditor.exe` in a directory of choice and create shortcuts on the desktop. In addition, the master zip file contains the following model files containing the models illustrated in this article:

2States.mod
LigandGated.mod
Patlak_Na-Channel.mod
Patlak_Na-Channel_Mut.mod
Uniporter.mod

These model files can be loaded via the Menu item `File->Open`.

Further, the following setting files are included

2States.set
LigandGated.set
LigandGatedLongSimulation.set
LigandGatedDwellTimeDistribution.set
NaChannelIV.set
UniporterVaryParams.set
UniporterVisualSimulation.set

Finally, the pulse generator file (`pgf`), `Pulses.pgf`, is included. It contains several sample stimulation protocols.

It is possible that some antivirus programs will recognize MarkovEditor as a virus. In this

case, you need to explicitly instruct your antivirus program that `MarkovEditor.exe` is not a virus.

Furthermore, because MarkovEditor is written in Visual C++, it necessitates several dll files from the Visual C++ redistribution suite. If these are not present on the computer, an error message appears on launching MarkovEditor. In this case you need to install these dlls by executing the program `vc_redist86.exe`, contained in the MarkovEditor master zip file. Now, MarkovEditor should run.

XXI. TUTORIAL 2: INSERTING THE 2-STATE MODEL INTO MARKOVEDITOR

MarkovEditor can hold several models simultaneously, each in its own window. Windows are divided in 2 panes: the upper pane show model predictions; the lower pane harbors the model itself. All models discussed in this article are contained in the master zip file that can be downloaded from <https://github.com/mikpusch/MarkovEditor.git>. These models can be loaded into the program via the menu item `File->Open`.

The following steps describe the manual creation of the 2-state model within MarkovEditor from a blank new file.

(a) Adding the states of the model

In the lower pane, double-click or right-click on empty space to create the closed and the open states. For each, assign a label (e.g., “C” to the closed state), a current value (for now, 0 for the closed state and 1 for the open state), and for now, ignore (i.e., assign default values by simply hitting ok) for sigma and initial probability function. Note that the index of state C is 0. In general, indices in MarkovEditor follow the convention of the C programming language to range from 0 to $N-1$ for an array of N items. A maximum of 100 states can be present in a single model.

(b) Assigning the parameters of the model

The voltage-dependent 2-state model is characterized by 4 parameters, α_0 and β_0 , z ,

and δ (see main text). Such parameters are held in an array that is accessed by clicking on the Parameters button in the lower pane of MarkovEditor, bringing up a dialog box in which values for up to 36 parameters (from $A[0]$ to $A[35]$) can be assigned.

Here, we will use in an arbitrary manner parameters $A[0]$ for α_0 , $A[1]$ for β_0 , $A[2]$ for z and $A[3]$ for δ assigning values:

$$A[0] = 10$$

$A[1] = 1$, meaning that at 0 mV, the closing rate is 10 times slower than the opening rate, implying that opening is favored, i.e., that $V_{1/2}$ is negative;

$A[2] = 2$, a gating valence of 2 elementary charges;

$A[3] = 0.5$, i.e., symmetric voltage dependence of opening and closing rate constants.

Next, to formulate the voltage-dependent rate constants, we add variables, which are expressions dependent on parameters $A[i]$, voltage (or concentration), and other variables that have been already defined. To this end, we click on the Variables button in the lower pane, select Add, and enter the following string in the dialog box

$A[0] \times \exp(v \times A[2] \times A[3] / 25)$ opening rate constant creating variable $w[0]$. This is exactly reflecting Eq. 17, defining the voltage-dependent opening rate constant ($V = \alpha_0 e^{\delta z V q_e / (kT)}$), i.e., $w[0] = \alpha(V)$.

Note that expressions are not case sensitive (i.e., no distinction is made between uppercase and lowercase characters) and that comments can be added after the defining expression preceded by `'`. The division by 25 (i.e., 25 mV) expresses that at ambient temperature the value of kT/q_e is around 25 mV. A maximum of 1,000 variables can be added to a model. We next add variable $w[1]$ by repeating the above procedure and inserting the string

$A[1] \times \exp(-v \times A[2] \times (1 - A[3]) / 25)$ closing rate constant

reflecting Eq. 18, which defines the voltage-dependent closing rate constant $\beta(V) = \beta_0 e^{-(1-\delta)zVq_e/(kT)}$, i.e., $w[1] = \beta(V)$.

To assign these variables as rate constants for state transitions, we right-click between the 2 states, select New transition 1 and insert the string

$w[0]$

in the dialog box. Next, we repeat the procedure now inserting

$w[1]$

as New transition 2. Then, we insert the voltage-dependent single-channel current of the open state, characterized by the single-channel conductance γ and the reversal potential E_{rev} . We delegate these parameters to $A[4]$ and $A[5]$, respectively, assigning values of 10 to $\gamma = A[4]$, reflecting a conductance of 10 pS, and -80 to $E_{rev} = A[5]$ reflecting a typical equilibrium potential of -80 mV of K^+ in excitable cells. To render this decision explicit, we define a novel variable $w[2]$ as follows:

$A[4] * (v - A[5]) * 1e-3$ single-channel current in pA

This expression needs 2 clarifications. First, the seemingly awkward string $1e-3$ (or equivalently $1E-3$, remember that these expressions are not case sensitive) is a convention used in C and other programming languages to enter the number 10^{-3} . For example, to enter the number -1.23×10^{-4} , one would use the string $-1.23E-4$. Second, the scaling by 10^{-3} reflects the choice to express voltage in millivolts, current in picoamperes and conductance in picosiemens. To assign this expression as the single channel current of state O , we right-click on state O , select EditState and enter $w[2]$ as *current*.

Finally, to render single-channel simulations more realistic, i.e., to make them look like real recordings (and to test the performance of single-channel analysis programs regarding noise), we add a noise level to each conductance state. This is used only for the stochastic simulations, not for the deterministic macroscopic predictions. To this end, we right-click again on each state and assign a certain noise value to the *sigma* field, resulting in the addition of white noise with standard deviation

given by the σ value (in picoamperes). For example we add a noise of 0.05 pA to the current of the closed state and a larger value of 0.1 pA to the open state to simulate the open channel noise seen experimentally for many channels (15). Now, the 2-state model is ready for exploration.

XXII. TUTORIAL 3: GENERAL SETTINGS

The general settings dialog is invoked by the menu click `Settings->Edit general settings`. Settings can be saved on file. Note that on start-up, MarkovEditor automatically loads the latest setting file that had been saved or loaded during previous sessions.

In the dialog, the Voltage Scaling tab defines the voltage or concentration range for which steady-state properties are to be calculated and plotted. The Probability Codes tabs define the states for which the occupation probabilities is plotted. The pulse protocol consists of 3 time segments. A holding segment of duration t_0 , and 2 segments for which not only the voltage and concentration and duration, but also increments (or decrements) for these values can be specified. The sample time determines the number of points to be calculated (and plotted). The time step in visual simulation (ms) determines the speed with which the visual simulation of a single transporter will be visualized.

In the Spectrum tab, the frequency range over which the power spectrum is calculated is defined. `No. Freq. points` is number of points created for the spectrum plot. The `No. Channels in stochastic simulations` is relevant only for stochastic simulations! For deterministic calculations, the number of channels is considered always 1.

XXIII. TUTORIAL 4: THE PGF STIMULATION PROTOCOLS

Selecting the menu item `Settings->Edit pgf file` opens the pgf dialog shown in Supplemental Figure S1. The same stimulation protocols are used in the GePulse data acquisition program (<https://github.com/mikpusch/GePulse.git>).

A sample pgf file called `Pulses.pgf` containing several stimulation protocols is included in the material that can be downloaded from <https://github.com/mikpusch/MarkovEditor.git>. Note that on start-up, MarkovEditor automatically loads the latest pgf file that had been saved or loaded during previous sessions.

The most important parameter for the stimulation protocol is the `sample interval` (in milliseconds), which determines the density of points to be calculated. Each stimulation consists of an arbitrary number of segments, which are created by clicking on the corresponding N (for new) button and deleted by clicking on the D (for delete) button. For each segment, the segment type has to be chosen among `VHOLD`, `CONSTANT`, `RAMP`, `SINE` or `WAVE`. Make sure to click on the selected text after selection to make the selection definite (it has to be shown in blue color)! The meaning of the segment types are the following.

VHOLD: The initial voltage (i.e., that of the first sweep) is determined by the holding voltage, which is defined in the General Settings (see Tutorial 3). In the GePulse acquisition program, `VHOLD` is defined in the front panel. Apart from the value of the initial voltage, the segment behaves like a `CONSTANT` segment.

CONSTANT: The voltage remains constant throughout the segment. Its (initial) duration is determined by the `Duration` field. If the number of sweeps is larger than 1, the increments `Delta V` and `Delta t` are applied to determine the voltage and duration of the segment in successive sweeps. The `V-factor` and `t-factor` are applied multiplicatively to increment (or decrement) voltage or time. In particular a `t-factor` of 1.5 is useful for so-called envelope protocols, such as recovery from inactivation of sodium channels. Initially, time increments are small, allowing precise sampling of the initial rapid phase and become exponentially longer, thereby reducing the number of pulses that have to be applied to reach long durations.

RAMP: The voltage changes linearly over time from the previous value (of the previous segment or `VHold`) to that defined in the voltage field.

SINE: The segment consists of a piece of a sine wave around the voltage defined in the voltage field, with frequency defined in the `f Sine` field and amplitude defined in the `v sine` field.

WAVE: An arbitrary shape of stimulation can be loaded from a text file. The file has to contain one number (i.e., voltage) per line. This is useful, for example, for stimulation with the shape of an action potential.

In MarkovEditor, the `Leak` tab, where the classical P/4 style leak subtraction can be defined, is not used. Also the `Chain` tab, with which in GePulse different stimulation protocols can be linked, is not used in MarkovEditor. In case the simulation is intended to be used also by the GePulse acquisition program, the `Relevant Seg` tab is useful to define the segment whose voltage is relevant for analysis (`Rel X Seg`) and the segment whose current level should be analyzed (`Rel Y Seg 1`).

To create a new stimulation sequence, click on an empty field on the top and assign a name. A `pgf` file can hold an arbitrary number of stimulation sequences, can be saved on disk by clicking on the `Save` button, and loaded from a disk by clicking on the `Load` button. Note that there is no warning if changes made have not been saved to the disk before exiting the program.

XXIV. TUTORIAL 5: GRAPH OPTIONS

For each model window, MarkovEditor keeps in memory several graphs illustrating the results of the last performed simulation. Each graph is populated once the `Calculate` or the `VaryParams` button is clicked. After changing any parameter of the model to update the graph, the `Calculate` or the `VaryParams` button has to be clicked again, i.e., graphs are not updated automatically after change of parameters.

Data shown in the graphs can be exported in ASCII format to the clipboard or to a text file by right-clicking on the graph. For some graphs (e.g., time course), data can also be exported in a binary format that can be opened by the Ana analysis program (<https://github.com/mikpusch/Ana.git>) and the GePulse data acquisition program (<https://github.com/mikpusch/GePulse.git>).

For each plot present in a graph, a short line of the same color is drawn on the top right of the graph. When the mouse pointer is placed close to such a short line, the corresponding plot will be drawn with a thick pen, and additional text related to the plot is displayed.

The axes can be in automatic or manual scale and either on a linear or a logarithmic scale. These settings can be changed by right-clicking on the axis. A variable number of ticks is shown.

XXV. TUTORIAL 6: EXPLORATION OF THE PARAMETER SPACE: THE VARY PARAMS DIALOG

MarkovEditor offers a systematic way to explore the behavior of the model when different values are assigned to the parameters encoded in the array fields `A[0] ... A[35]`. The variation scheme is accessed by the menu item `Settings->Edit vary which params`. In the dialog, up to 8 parameters can be selected to be varied. For each chosen parameter, several options can be selected: a lower and an upper bound, the number of steps, and if variation should be done on a logarithmic scale. For example, to explore values 0.1, 1, and 10 for parameter `A[0]`, the lower bound is 0.1, the upper bound 10, the number of steps 3, and variation is to be done on a logarithmic scale.

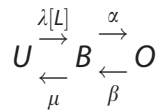
XXVI. TUTORIAL 7: ENTERING THE 3-STATE, LIGAND-ACTIVATED CHANNEL MODEL

All models discussed in this article are contained in the master zip file that can be downloaded from <https://github.com/mikpusch/MarkovEditor.git>. These models can

be loaded into the program via the menu item `File->Open`. In particular, the ligand activated 3-state model is contained in the file `LigandGated.mod`.

However, to provide an additional example highlighting the logic behind MarkovEditor, the following steps describe the manual creation of the 3-state ligand gated model within MarkovEditor from a blank new file.

The model



is characterized by 5 parameters: λ , $[L]$, μ , α , and β . The ligand concentration $[L]$ could be encoded by one of the parameters, e.g., following a certain tradition of MarkovEditor, encoding it in parameter `A[32]`. Alternatively, and this will be done here, instead of using the voltage as the dominant variable determining channel behavior, the concentration of the ligand, denoted as c , will be used as the independent variable, playing an equivalent role as the voltage in voltage-gated channels. This will allow us to easily construct dose-response curves as well as concentration jump experiments. Parameters λ , μ , α , and β are delegated to `A[0]`, `A[1]`, `A[2]`, `A[3]` respectively, assigning, for example, `A[0]=A[1]=1` and `A[2]=A[3]=2`.

To create a new model, the `File->New` menu option can be selected and the previously mentioned parameters values are entered by clicking on the `Parameters` button in the lower pane. States U , B , and O are created by double-clicking or right-clicking in empty space. As for the 2-state model, to render single-channel simulations realistic, we assign a `sigma` value of 0.1 to all states. The current is 0 for states U and B and 1 for state O . The ligand concentration $[L]$ will be entered as c , instead of the variable v used for voltage-gated channels. For the simple model we will not use any variable but insert the various transition rate constants by right-clicking between states and entering `A[0] * c` for the rate constant from state U to state B and the strings `A[1]`, `A[2]`, `A[3]` for the remaining transitions, respectively.

See Supplemental Figure S2 for a screenshot of the final model.

We also adjust the general settings by choosing `cLeft = 0.01`, `cRight = 10`, `deltaC = 0.01`, where `cLeft` is the lowest, and `cRight` the highest concentration to be plotted in the graph displaying the steady-state concentration dependence, with points separated by steps of `deltaC`. We next impose the following pulse protocol `Npulses=1`, `sample time=10`, `cHold=0.01`, `c1=2`, `c2=0.01`, `t0=1000`, `t1=10000`, `t2=5000`. This pulse emulates a concentration jump from a very low concentration (0.01 mM) to a high concentration (2 mM) and back to 0.01 mM. Do not forget to save the model (`File->Save`) and the settings (`Settings->Save`) on disk. The corresponding model file (`LigandGated.mod`) and settings file (`LigandGated.set`) can also be downloaded from <https://github.com/mikpusch/MarkovEditor.git>.

XXVII. TUTORIAL 8: ENTERING PATLAK MODEL OF VOLTAGE-GATED Na^+ CHANNELS—THE TEXT-BASED INTERFACE

We will enter model 7 of (23) by using the text-based interface of MarkovEditor. To this end, we first create a new and empty model by selecting `File->New`. Now, we right-click in the lower window, and from the pop-up menu, we select `Edit model in text window`, which will open a text window. Here, we delete all text present (right-click and chose `Select all` and after that `Delete` from the pop-up menu) and paste (right-click and select `Paste` from the pop-up menu) the following text exactly as shown:

```

TRANSPORTER-GATING CURRENT
FUNCTION:auto
FUNCTIONS:
FUNC[0]=x*a[13]/(x+a[13]) ' used to
keep rate constants below upper
limit a[13]
VARIABLES:
w[0]=log(6.24e12) ' ln(kT/h) - model
7 from Patlak, Physiol. Rev. 1991

```

```

w[1]=exp(w[0] + a[4] + (1-a[8]) * a[6] + a[7] * a[8] * v/25) ' kappa
w[2]=exp(w[0] + a[5] + a[8] * a[6] - a[7] * (1-a[8]) * v/25) ' lambda
w[3]=exp(w[0] + a[0] + a[7] * a[8] * v/25) ' alpha_m
w[4]=exp(w[0] + a[1] - a[7] * (1-a[8]) * v/25) ' bet_am
w[5]=exp(w[0] + a[2] + a[8] * a[6] + a[7] * a[8] * v/25) ' delta
w[6]=exp(w[0] + a[3] + (1-a[8]) * a[6] - a[7] * (1-a[8]) * v/25) ' gamma
w[7]=exp(w[0] + a[9] - a[11] * (1-a[12]) * v/25) ' alpha_h
w[8]=exp(w[0] + a[10] + a[11] * a[12] * v/25) ' beta_h
STATES:
#0;C1; i=0; sigma =0.05; initprob =1; x = 1.9089574e-002; y = 0.28961749
#1;C2; i=0; sigma =0.05; initprob =1; x = 0.22393539; y = 0.29143898
#2;C3; i=0; sigma =0.05; initprob =1; x = 0.3773862; y = 0.29143898
#3;C4; i=0; sigma =0.05; initprob =1; x = 0.55506608; y = 0.29143898
#4;O; i=0.01*(v-50); sigma =0.05; initprob =1; x = 0.79368576; y = 0.29326047
#5;I1; i=0; sigma =0.05; initprob =1; x = 0.55580029; y = 0.77595628
#6;I2; i=0; sigma =0.05; initprob =1; x = 0.79295154; y = 0.7704918
RATES:
FROM 0 TO 1:func[0] (4* w[1] )
FROM 1 TO 0:func[0] (w[2] )
FROM 1 TO 2:func[0] (3* w[3] )
FROM 2 TO 1:func[0] (2* w[4] )
FROM 2 TO 3:func[0] (2* w[3] )
FROM 3 TO 2:func[0] (3* w[4] )
FROM 3 TO 4:func[0] (4* w[5] )
FROM 3 TO 5:func[0] (w[8] )
FROM 4 TO 3:func[0] (w[6] )
FROM 4 TO 6:func[0] (w[8] )
FROM 5 TO 3:func[0] (w[7] )
FROM 5 TO 6:func[0] (4* w[5] ) ' 4* delta
FROM 6 TO 4:func[0] (w[7] )
FROM 6 TO 5:func[0] (w[6] )
PARAMETERS:
a[0]=-19.
a[1]=-22.35
a[2]=-19.
a[3]=-23.9
a[4]=-21.32
a[5]=-27.08
a[6]=-1.8
a[7]=2.45
a[8]=0.6
a[9]=-26.5
a[10]=-22.4
a[11]=0.3
a[12]=0.5
a[13]=20000

```

Now, right-click again and select `Parse` from the pop-up menu. If no error occurred (which should be the case for the previously mentioned code), a message saying `Successfully parsed and copied into model` should appear, signaling that everything went smoothly and that you can safely close the text window. The model should correctly appear, as illustrated in Figure 6A.

XXVIII. TUTORIAL 9: MANUAL DEFINITION OF THE GATING CURRENT FUNCTION FOR THE 2-STATE MODEL

To illustrate the general use of the `Transporter/gating current` function, we will define a function that allows to calculate gating currents of the 2-state model defined in Eq. 1 and rate constants defined in Eqs. 17 and 18.

According to Eq. 29, gating currents for the 2-state model are given by

$$I_{\text{gate}}(t) = q_e z (p_C(t) \alpha - p_O(t) \beta)$$

Thus, having implemented the 2-state model in `MarkovEditor`, as described in Tutorial 1, using the variables `w[0]` and `w[1]` for the rate constants, and `a[2]` for the gating valence, the `Transporter/gating current` function can be inserted as

```
1.6e-19* a[2] * (p[0] * w[0] - p[1] * w[1]) /
1e-12 ' gating current in pA
```

that gives the gating current in picoamperes. This should give the same result as the automatic mode, i.e., inserting `auto` as the `Transporter/gating current` function.

XXIX. TUTORIAL 10: INSERTING THE UNIORTER MODEL INTO MARKOVEDITOR

As in Tutorial 8, we will enter the uniporter model by using the text-based interface of MarkovEditor. To this end, we first create a new and empty model by selecting `File->New`. Now, we right-click in the lower window, and from the pop-up menu, we select `Edit model` in text window, which will open a text window. Here, we delete all text present (right-click and chose `Select all` and after that `Delete` from the pop-up menu) and paste (right-click and select `Paste` from the pop-up menu) the following text exactly as shown:

```
TRANSPORTER-GATING CURRENT
FUNCTION: auto
FUNCTIONS:
VARIABLES:
w[0] =a[4] * exp (-v* a[0] /2/25) ' empty
transporter moves inward
w[1] =a[4] * a[7] / a[6] ' obey
microscopic reversibility
w[2] =w[1] * exp (v* a[0] /2/25) ' empty
transporter moves outward
w[3] =a[6] * exp (-v* (a[2] +a[0] )/2/25) '
loaded transporter moves inward
w[4] =a[7] * exp (v* (a[2] +a[0] )/2/25) '
loaded transporter moves outward
w[5] =a[8] * exp (v* a[1] /2/25) '
unbinding of substrate to the
outside
w[6] =a[8] * exp (-v* (1-a[1] -a[2] )/2/
25) ' unbinding of substrate to the
inside
w[7] =a[9] * a[32] * exp (-v* a[1] /2/25) '
binding of substrate from outside
w[8] =a[9] * a[33] * exp (v* (1-a[1] -a[2] )/
2/25) ' binding of substrate from
inside
STATES:
#0;Out-0; i=0; sigma =0; initprob
=1; x = 0.50848896; y = 0.81777778
```

```
#1;In 0; i=0; sigma=0; initprob=1; x
= 0.52276065; y = 0.31554524
#2;Out 1; i=0; sigma=0; initprob=1;
x = 0.72099853; y = 0.80046404
#3;In 1; i=0; sigma=0; initprob=1; x
= 0.73568282; y = 0.32018561
```

RATES:

```
FROM 0 TO 1:w[0]
FROM 0 TO 2:w[7]
FROM 1 TO 0:w[2]
FROM 1 TO 3:w[8]
FROM 2 TO 0:w[5]
FROM 2 TO 3:w[3]
FROM 3 TO 1:w[6]
FROM 3 TO 2:w[4]
```

PARAMETERS:

```
a[0] =-0.1
a[1] =0.2
a[2] =0.5
a[4] =100.
a[6] =100.
a[7] =100.
a[8] =1000.
a[9] =1000.
a[32] =1.
a[33] =1.
```

Now, right-click again and select `Parse` from the pop-up menu. If no error occurred (which should be the case for the previously mentioned code), a message saying `Successfully parsed and copied into model` should appear, signaling that everything went smoothly and that you can safely close the text window.

ACKNOWLEDGMENTS

MP is supported by a grant from the Fondazione Associazione Italiana Ricerca sul Cancro (AIRC) per la Ricerca sul Cancro (grant IG 21558) and the Italian Research Ministry (PRIN 20174TB8KW). Feel free to contact the authors at michael.pusch@cnr.it.

AUTHOR CONTRIBUTIONS

MP designed and implemented the program, and all authors contributed to manuscript writing.

REFERENCES

1. Wagoner, J. A., and K. A. Dill. 2019. Opposing pressures of speed and efficiency guide the evolution of molecular machines. *Mol Biol Evol* 36(12):2813–2822.

2. Science ABC. 2019. The human brain vs. supercomputers...which one wins. Accessed 1 Oct 2020. <https://www.scienceabc.com/humans/the-human-brain-vs-supercomputers-which-one-wins.html>.
3. Neher, E., and B. Sakmann. 1976. Single-channel currents recorded from membrane of denervated frog muscle fibres. *Nature* 260(5554):799–802.
4. Schein, S. J., M. Colombini, and A. Finkelstein. 1976. Reconstitution in planar lipid bilayers of a voltage-dependent anion-selective channel obtained from paramecium mitochondria. *J Membr Biol* 30(2):99–120.
5. Hamill, O. P., A. Marty, E. Neher, B. Sakmann, and F. J. Sigworth. 1981. Improved patch-clamp techniques for high-resolution current recording from cells and cell-free membrane patches. *Pflügers Arch* 391(2):85–100.
6. Hille, B. 2001. *Ion Channels of Excitable Membranes*. Sinauer, Sunderland, MA.
7. Hodgkin, A. L., and A. F. Huxley. 1952. A quantitative description of membrane current and its application to conduction and excitation in nerve. *J Physiol* 117(4):500–544.
8. Jiang, Y., A. Lee, J. Chen, V. Ruta, M. Cadene, B. T. Chait, and R. MacKinnon. 2003. X-ray structure of a voltage-dependent K⁺ channel. *Nature* 423(6935):33–41.
9. Long, S. B., E. B. Campbell, and R. MacKinnon. 2005. Crystal structure of a mammalian voltage-dependent Shaker family K⁺ channel. *Science* 309(5736):897–903.
10. Colquhoun, D., and A. G. Hawkes. 1981. On the stochastic properties of single ion channels. *Proc R Soc Lond B Biol Sci* 211(1183):205–235.
11. Sakmann, B., and E. Neher. 1995. *Single-Channel Recording*. Springer, New York.
12. Johnston, D., and S. M.-S. Wu. 1994. *Foundations of Cellular Neurophysiology*. The MIT Press, Cambridge, MA.
13. Colquhoun, D., C. J. Hatton, and A. G. Hawkes. 2003. The quality of maximum likelihood estimates of ion channel rate constants. *J Physiol* 547(3):699–728.
14. Sigg, D. 2014. Modeling ion channels: past, present, and future. *J Gen Physiol* 144(1):7–26.
15. Sigworth, F. J. 1985. Open channel noise. I. Noise in acetylcholine receptor currents suggests conformational fluctuations. *Biophys J* 47(5):709–720.
16. DeFelice, L. J. 1981. *Introduction to membrane noise*. Plenum Press, New York.
17. Chen, Y. D., and T. L. Hill. 1973. Fluctuations and noise in kinetic systems. Application to K⁺ channels in the squid axon. *Biophys J* 13(12):1276–1295.
18. Conti, F., and E. Wanke. 1975. Channel noise in nerve membranes and lipid bilayers. *Q Rev Biophys* 8(4):451–506.
19. Colquhoun, D., and A. G. Hawkes. 1990. Stochastic properties of ion channel openings and bursts in a membrane patch that contains two channels: evidence concerning the number of channels present when a record containing only single openings is observed. *Proc R Soc Lond B Biol Sci* 240(1299):453–477.
20. Colquhoun, D., and F. J. Sigworth. 1995. Fitting and statistical analysis of single-channel records. In *Single-Channel Recording*. B. Sakmann and E. Neher, editors. Plenum Press, New York, pp. 483–585.
21. Qin, F., A. Auerbach, and F. Sachs. 1996. Estimating single-channel kinetic parameters from idealized patch-clamp data containing missed events. *Biophys J* 70(1):264–280.
22. Epstein, M., B. Calderhead, M. A. Girolami, and L. G. Sivilotti. 2016. Bayesian statistical inference in ion-channel models with exact missed event correction. *Biophys J* 111(2):333–348.
23. Patlak, J. 1991. Molecular kinetics of voltage-dependent Na⁺ channels. *Physiol Rev* 71(4):1047–1080.
24. Ahern, C. A., J. Payandeh, F. Bosmans, and B. Chanda. 2016. The hitchhiker's guide to the voltage-gated sodium channel galaxy. *J Gen Physiol* 147(1):1–24.
25. Bezanilla, F. 2018. Gating currents. *J Gen Physiol* 150(7):911–932.
26. Conti, F., and W. Stühmer. 1989. Quantal charge redistributions accompanying the structural transitions of sodium channels. *Eur Biophys J* 17(2):53–59.
27. Cannon, S. C. 2000. Spectrum of sodium channel disturbances in the nondystrophic myotonias and periodic paralyses. *Kidney Int* 57(3):772–779.
28. Catterall, W. A. 2000. From ionic currents to molecular mechanisms: the structure and function of voltage-gated sodium channels. *Neuron* 26(1):13–25.
29. Hayward, L. J., R. H. Brown, Jr., and S. C. Cannon. 1996. Inactivation defects caused by myotonia-associated mutations in the sodium channel III-IV linker. *J Gen Physiol* 107(5):559–576.
30. Bertelli, S., R. Barbieri, M. Pusch, and P. Gavazzo. 2018. Gain of function of sporadic/familial hemiplegic migraine-causing SCN1A mutations: use of an optimized cDNA. *Cephalalgia* 39(4):477–488.
31. Barbieri, R., S. Bertelli, M. Pusch, and P. Gavazzo. 2019. Late sodium current blocker GS967 inhibits persistent currents induced by familial hemiplegic migraine type 3 mutations of the SCN1A gene. *J Headache Pain* 20:107. <https://doi.org/10.1186/s10194-019-1056-2>.
32. Gadsby, D. C., F. Bezanilla, R. F. Rakowski, P. De Weer, and M. Holmgren. 2012. The dynamic relationships between the three events that release individual Na⁽⁺⁾ ions from the Na⁽⁺⁾/K⁽⁺⁾-ATPase. *Nat Commun* 3:669. <https://doi.org/10.1038/ncomms1673>.
33. Läuger, P. 1991. *Electrogenic Ion Pumps*. Sinauer, Sunderland, MA.
34. Frehland, E. 1978. Current noise around steady states in discrete transport systems. *Biophys Chem* 8(3):255–265.
35. Kolb, H. A., and E. Frehland. 1980. Noise-current generated by carrier-mediated ion transport at non-equilibrium. *Biophys Chem* 12(1):21–34.
36. Hill, T. L. 1977. *Free Energy Transduction in Biology*. Academic Press, New York.
37. Ruivo, R., G. C. Belenchi, X. Chen, G. Zifarelli, C. Sagne, C. Debacker, M. Pusch, S. Supplisson, and B. Gasnier. 2012. Mechanism of proton/substrate coupling in the heptahelical lysosomal transporter cystinosin. *Proc Natl Acad Sci U S A* 109(5):E210–E217.
38. Akyuz, N., R. B. Altman, S. C. Blanchard, and O. Boudker. 2013. Transport dynamics in a glutamate transporter homologue. *Nature* 502(7469):114–118.
39. Richard, E. A., and C. Miller. 1990. Steady-state coupling of ion-channel conformations to a transmembrane ion gradient. *Science* 247(4947):1208–1210.
40. Press, W. H., S. A. Teukolsky, W. T. Vetterling, and B. P. Flannery. 2007. *Numerical Recipes in C: The Art of Scientific Computing*. Cambridge University Press, Cambridge.